GA-C19465
6/90

HIGH TEMPERATURE CERAMIC SUPERCONDUCTORS

FOR PERIOD
APRIL 1, 1990 – JUNE 30, 1990

AD-A224 847

Prepared for
OFFICE OF NAVAL RESEARCH
800 North Quincy Street
Arlington, VA 22217-5000
DARPA/ONR Contract N00014-88-C-0714

Prepared by
K.S. MAZDIYASNI, PROGRAM MANAGER (619) 455-4587
A. CHEN
K.C. CHEN
D.M. DUGGAN
F.C. MONTGOMERY
S.S. PAK
M.B. MAPLE, UCSD
L. PAULIUS, UCSD
P. TSAI, UCSD

APPROVED BY: _T.D. Gulden_
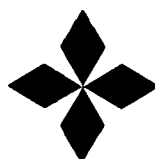
T.D. GULDEN
DIRECTOR, DEFENSE MATERIALS

The views and conclusions contained in this quarterly report are those of the authors and should not be interpreted as necessarily representing the official policies, either expressed or implied, of the Defense Advanced Research Project Agency of the U.S. Government.

GENERAL ATOMICS PROJECT 3850

◆ GENERAL ATOMICS

90 07 26 071

CONTENTS

FIGURES

FIGURES (Continued)

TABLES

1. INTRODUCTION

This is the sixth quarterly progress report on the work performed in the period from April 1, 1990 through June 30, 1990 on Office of Naval Research (ONR) Contract N00014-88-C-0714, entitled "High-Temperature Ceramic Superconductors." The principal objectives of this program are (1) to demonstrate fabrication of high-temperature ceramic superconductors that can operate at or above 90 K with appropriate current density, J_c, in forms useful for application in resonant cavities, magnets, motors, sensors, computers, and other devices; and (2) to fabricate and demonstrate selected components made of these materials, including microwave cavities and magnetic shields.

1.1. PROJECT OUTLINE

This program consists of six tasks: (1) metal alkoxide synthesis and processing, (2) microstructural evaluation and property measurement, (3) electrical and magnetic property measurement, (4) superconductor ceramic processing, (5) component fabrication and demonstration, and (6) reporting.

Task 1 is to synthesize a homogeneous alkoxide solution that contains all the constituent elements that can be easily made into powders, thin film, or drawn into fiber form. Ideally, this solution should possess precise stoichiometry, adequate stability, polymerizability, adherence, and spinnability. Also, the polymeric materials formed from this solution should be thermosetting, be able to be dissolved in organic solvents, and contain as little as possible low-temperature pyrolyzable organics with high char yield.

Task 2 is to study the microstructure as a function of processing parameters. The study includes: density, pore size, and pore size distribution, phase identification, chemical composition and purity, environmental stability, effects of heat treatment, residual strain, seeding, annealing in magnetic fields, and epitaxy on grain growth and orientation.

Task 3 is to study the electrical and magnetic properties of the $YBa_2Cu_3O_7$ (123) high T_c ceramic superconductors. It will include both the ac electrical resistance (R_{ax}) and the ac magnetic susceptibility (χac).

Task 4 is to investigate superconductor ceramic processing. Most of the important applications of superconductors require material in the form of fiber or films. Magnets, conductors, motors, and generators are examples of applications employing fiber; while detectors, microwave cavities, and microcircuitry require superconducting material in the form of films. The sol-gel process is ideally suited to producing materials in these forms; in fact, it is used commercially to produce ant-reflection and mirror coatings and to produce continuous ceramic fibers for structural reinforcement in composite materials and for thermal insulation.

Task 5 is to demonstrate component fabrication. General Atomics (GA) will design and build a high Q, high Tc superconducting cavity, using its unique sol-gel coating process capabilities. This task will proceed after some initial coating tests have verified dc superconductivity and after we have answered questions of adhesiveness, surface preparation, and processing procedures. As the fabrication process and the materials quality are improved throughout the three-year program, two additional cavities will be constructed and tested. Coupling will be through a waveguide inductive iris into an end wall, with a logarithmic decrement technique of Q measurement considered most appropriate

for the high Q anticipated. An X-band (10 GHz) frequency choice allows for convenient dimensions of 4.3 cm diameter by 2.8 cm height.

This report will focus primarily on Tasks 2, 3, 4, and 5.

	DEVELOPMENT OF HIGH TEMPERATURE T_c SUPERCONDUCTOR			
ACTIVITY	FY 1988	FY 1989	FY 1990	FY 1991
	M J J A S	O N D J F M A M J J A S	O N D J F M A M J J A S	O N D J F M A
TASK 1 METAL ALKOXIDE SYNTHESIS AND PROCESSING				
SUPERCONDUCTIVITY TECHNICAL ASSESSMENT				
THEORY AND ANALYSIS				
MATERIAL SELECTION				
PRECURSOR SYNTHESIS				
SOL-GEL PROCESSING				
MATERIAL PROCESSING FLOWSHEETS				
MATERIAL PROCESSING CHARACTERIZATION				
TASK 2 MICROSTRUCTURE EVALUATION AND PROPERTY MEASUREMENT				
SPECIMEN FABRICATION				
CRYSTAL CHEMISTRY AND MATERIAL STRUCTURE				
PHASE IDENTIFICATION				
MATERIAL PROCESSING SELECTION				
MATERIAL CHARACTERIZATION				
TASK 3 ELECTRICAL AND MAGNETIC PROPERTY DETERMINATION				
BASIC SUPERCONDUCTOR MAGNETIC PROPERTY MEASUREMENT				
THEORY AND ANALYSIS				
MATERIAL SELECTION				
TASK 4 SUPERCONDUCTOR CERAMIC PROCESSING				
PROCESS PARAMETER STUDY				
MATERIAL FABRICATION POWDER FILM FIBER				
MATERIAL CHARACTERIZATION STRUCTURE AND ELECTRICAL MAGNETIC PROPERTIES				
MANUFACTURING PROCESS FLOWSHEET OPTIMIZATION				
TASK 5 COMPONENT FABRICATION AND DEMONSTRATION				
TASK 6 PROGRAM DELIVERABLES				

J-358(1)
J-18-90

▼ DELIVERABLES

2. THIN FILM AND FIBER PROCESSING

During this reporting period, two types of metal organics were used to develop 123 films on different substrates.

Homogeneous solutions have been prepared using $Y(OR)_3$, $Ba(OR)_2$, and the copper (II) mixed-ligand species $(C_3H_7O_2)_2Cu_2(u-OR)_2$, where R = $CH_2CH_2OCH_2CH_2OCH_2CH_3$ and $C_5H_7O_2$ = 2,4-pentanedionate (Ref. 1).

2.1. EXPERIMENTAL PROCEDURES

The starting alkoxides, and the mixed-ligand copper (II) compound were prepared using the procedure described in a previous progress report under this effort.

2.1.1. Preparation of 123 Precursor Solution

In order to determine the stoichiometry and processing effects on the electrical properties of superconducting films, four precursor solutions (Table 1) were prepared following the procedure described in the January 1, 1990 to March 31, 1990, progress report (Ref. 2). The Y:Ba:Cu stoichiometry was varied in three of the solutions. The fourth solution was treated with hydrogen peroxide during the hydrolysis step.

2.1.2. Dip Coating

Dip coating was accomplished using the GA bench top dip coater.

2.1.3. Electrical Property Measurements

Resistance measurements were conducted at University of California, San Diego (UCSD) using a Linear Research LR-400 Four Wire ac Resistance

TABLE 1
STOICHIOMETRY OF HOMOGENEOUS SOLUTIONS
USED TO DIP COAT SUBSTRATES

Solution	Stoichiometry Molar Ratio			Hydrolysis Conditions	
	Y	Ba	Cu	H_2O	H_2O_2
10208-55	1.000	2.000	3.000	1.000	--
10208-83	1.028	2.000	2.998	1.003	--
10208-79	1.029	2.000	3.167	1.652	--
10208-97	1.028	2.000	2.994	1.003	0.198

Bridge, with a current of 0.1 uA at 13 Hz. Silver wire leads were cemented to the 123 film with silver paste after sputtering 1 mm x 3 mm silver pads on the coating. The pads were positioned by preparing an aluminum foil mask which surrounded the sample piece. The current pads were spaced 1 mm from the voltage pads, and the voltage pads were 4 mm apart. Thus, about 12 mm^2 of the film was tested.

As stated in Section 2.1.2, we have been investigating the effect that processing parameters have on the superconducting resistive transition. Figure 1 shows the general characteristics of the transition from the normal state to the superconducting state for films prepared on yttria-stabilized zirconia polycrystals (YSZP). The electrical resistance of the films decrease as the sample is cooled from room temperature. Near the transition temperature, the resistance drops rapidly and approaches zero within a range of a few degrees K. However, the minimum resistance of the films, with voltage leads spaced 4 mm apart, was only 0.07 ohm.

In order to compare the effects of processing conditions on the transition, three parameters describing the transition can be defined. These parameters (T_{90}, T_{50}, T_{10}) are the temperatures (K) at which the Resistance is 90%, 50%, and 10% of the value extrapolated from decreasing resistance in the normal state. The width of the transition is, then, $T_{90} - T_{10}$. Furthermore, a symmetric transition would have the same number of degrees between T_{90} and T_{50} as there are between T_{50} and T_{10}. Table 2 summarizes the processing conditions and the transition parameeters for several films made using the solutions in Table 1. In addition, the normal state resistance at 100 K is also given in Table 2.

The first two results in Table 2 show that the thickness of the film affects the transition. Based on the weight of material deposited, the thickness of the film produced by four dips is 1 to 2 um. Thus, the film dipped once would be 0.25 to 0.5 um thick. The thicker film results in a sharper transition from the normal to the superconducting
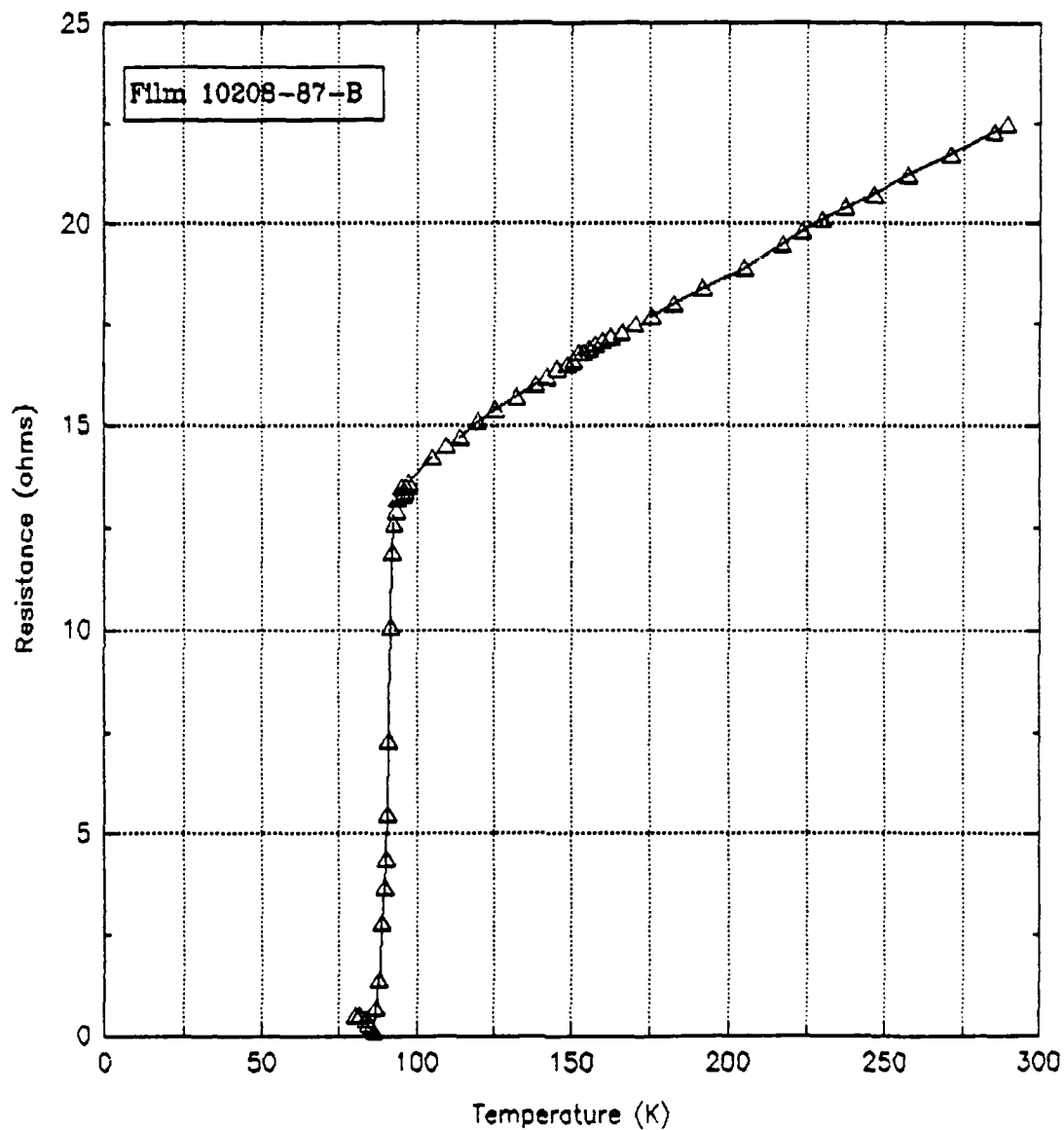
Fig. 1. Resistance as a function of temperature for an $YBaCO_{(7-x)}$ film on YSZP

TABLE 2
EFFECT OF PROCESSING PARAMEATERS ON THE
SUPERCONDUCTING TRANSITION PARAMETERS

Coating ID	Solution ID	Dip	Process	R100 ohms	T90 (K)	T50 (K)	T10 (K)
10208-105C	10208-83	4	$t_{max} = 902$[a] $t_{min} = 406$	15.8	93	91	87
10208-105E	10208-83	1	$t_{max} = 902$[a] $t_{min} = 406$	41.9	92	89	78
10208-72C	10208-55	4	$t_{max} = 905$[a] $t_{min} = 404$	17.1	92	90	85
10208-87C	10208-79	4	$t_{max} = 905$[a] $t_{min} = 404$	21.2	92	90	84
10208-87B	10208-83	4	$t_{max} = 905$[a] $t_{min} = 404$	14.6	92	91	87
10208-90B	10208-83	4	$t_{max} = 911$[a] $t_{min} = 402$	24.7	92	91	86
10208-90D	10208-79	4	$t_{max} = 911$[a] $t_{min} = 402$	8.3	92	91	88
10208-105B	10208-83	4	$t_{max} = 921$[a] $t_{min} = 405$	16.3	92.5	91	88
10208-116D	10208-83	4	(b)	9.9	93.8	90.8	87.3
10208-105A	10208-97	4	$t_{max} = 921$[b] $t_{min} = 405$	9.5	93.2	91.4	89.1
10208-117B	10208-97	4	(b)	8.3	92.9	90.6	86
10204-18A	10208-97	4	(c)	25.5	92.5	91.5	85

[a] 1°C/min to t_{max}; hold 10 min; 5°C/min to t_{min} hold 24 h.

[b] 5°C/min to 70; 1°C/min to 902; hold 10 min; 5°C/min to 500; 1°C/min to 403, hold 60 min.

[c] 1°C/min to 800; 0.5°C/min to 905; hold 10 min; 5°C/min to 404; hole 12 h.

state, and significantly lowers the initial resistance of the normal
state. Currently, we feel that this is being caused by reaction of a
certain volume of the film with the substrate.

In investigations of thin film deposition by various techniques,
the detrimental effects of superconductor-substrate interactions have
been reported (Ref. 3). The reaction of 123 (Y:Ba:Cu) with ZrO_2 is
known to occur at temperatures as low as 600°C and at 945°C results in
the formation of CuO, $BaZrO_3$ and the 211 compound (Ref. 4).

A preliminary observation indicating that reaction with the YSZP
substrate may be occurring during the processing of sol-gel derived
films from solution 10208-55 is given in Fig. 2. The transition in this
film began at 93 K and had a $T_{90} - T_{10}$ width of 16 K. The SEM photo-
micrograph shows the morphology of the film which had been processed
following the (a) procedure in the footnotes to Table 2 with t_{max} =
921°C. After a short etch with dilute HCl in methanol, two distinct
layers are evident in the thick portion of the film at the bottom of the
substrate. EDAX analysis of top layer (Y:Ba:Cu = 1.26:2.07:3.00) agreed
with microprobe analysis (1.24:2.11:3.00) of specific areas on the
surface of a film made from the same precursor solution 910208-55). The
lower layer seems to be enriched in copper although broadening of the
electron beam could have distorted the measurement of the compositional
difference.

Also, the stoichiometry of the solution affects the sharpness of
the superconducting transition of the film. The superconducting transi-
tions for films prepared from the solutions in Table 1 have a T_{90} of
about 92 K. However, the magnitude of the foot on the transition is
different for each solution. Microprobe analysis of the surface of the
films indicates that the surface is not single phase 123. Instead, the
films have areas with the correct stoichiometry interspersed with a

Fig. 2.   SEM photomicrograph showing morphology of superconducting
          film and apparent reaction layer

phase that has the proper Ba:Cu ratio but is high in yttrium. In addition, there are some spots that are high in yttrium and depleted in copper. We are currently trying to eliminate these segregated areas.

Increasing the processing temperature does not have a large effect on the resistance of the film. The width of the transitions for films prepared from solution 10208-83 which were heated to 905, 911, and 921°C (±2°C) were similar. However, the resistance of the normal state at 100 K was higher for the 911°C processed film. The cause of variability of the high resistance of these films are not known at this time and are being investigated by analytical electron microscopy work in an attempt to understand and correlate the microstructure processing properties relationships.

Earlier in this program we found the H_2O_2 added to the hydrolysis solution resulted in a 123 powder that did not contain any low melting (<980°C) phase. Thus, solution 1028-97 was prepared using H_2O_2 during hydrolysis. The electrical properties of the films prepared from this solution were similar to those prepared without the additive.

Several entries in Table 2 show the resistance transition of films from the same solution processed in three different ways. The samples that were cooled slowly between 500°C and 403°C with only a 1 h hold had the same properties as did the samples oxygenated for a longer time. Thus a 24-h oxygenation may not be required to obtain a sharp resistance drop at 92 K.

The rate at which the sample is heated to about 800°C does appear to affect the magnitude of the 100 K resistance. The resistance of the film that was heated at 0.5°C/min was about three times higher than a similar film heated twice as rapidly to the same maximum temperature.

2.1.4. 123 Film on SrTiO₃

Thin films of Y123 were prepared by dipping single crystal $SrTiO_3$ in a sol of the 123 resin in toluene and i-PrOH which currently has been used to make 123 fibers. The concentration of the resin was approximately 30 w/o and the ratio of toluene to i-PrOH was 4:1. The substrate was multiply dipped in air and pyrolyzed at 500°C in between each dip. Thus obtained film was fired at 825°C for 1 min in flowing O_2. The purpose of low temperature and short time firing was to minimize the chemical reaction between the substrate and the film. The film was fully oxygenated by holding at 400°C for 19 h in flowing O_2 atmosphere.

As the resistance curve (Fig. 3) shows, the film exhibited a metallic characteristic. The measured Tc was approximately 80 K and Jc =400 A/cm² at 30 K at 0 field. The XRD pattern (Fig. 4) shows the film is highly oriented with its c-axis perpendicular to the substrate surface. The Jc value is anticipated to be much higher than observed because the film thickness was not measured accurately. The Jc calculation was made by overestimation, using an arbitrary film thickness of 1 μm. It is expected that the Jc is to improve drastically with further work on processing optimization. For example, the SEM photograph (Fig. 5) shows the film is still quite porous and not fully crystalline.

2.2. 123 FILM ON SILVER (Ag)

With superconductivity well demonstrated using the present system on $SrTiO_3$, the next task was to demonstrate the same on more practical substrates such as polycrystalline Ag and yttria-stabilized zirconia polycrystals (YSZP). Since it is crucial to develop a highly dense and smooth film for the high Q cavity, it was necessary to determine the right heat treatment schedule for full densification and the attainment of fine grain size. Because of its inertness and thereby the absence of
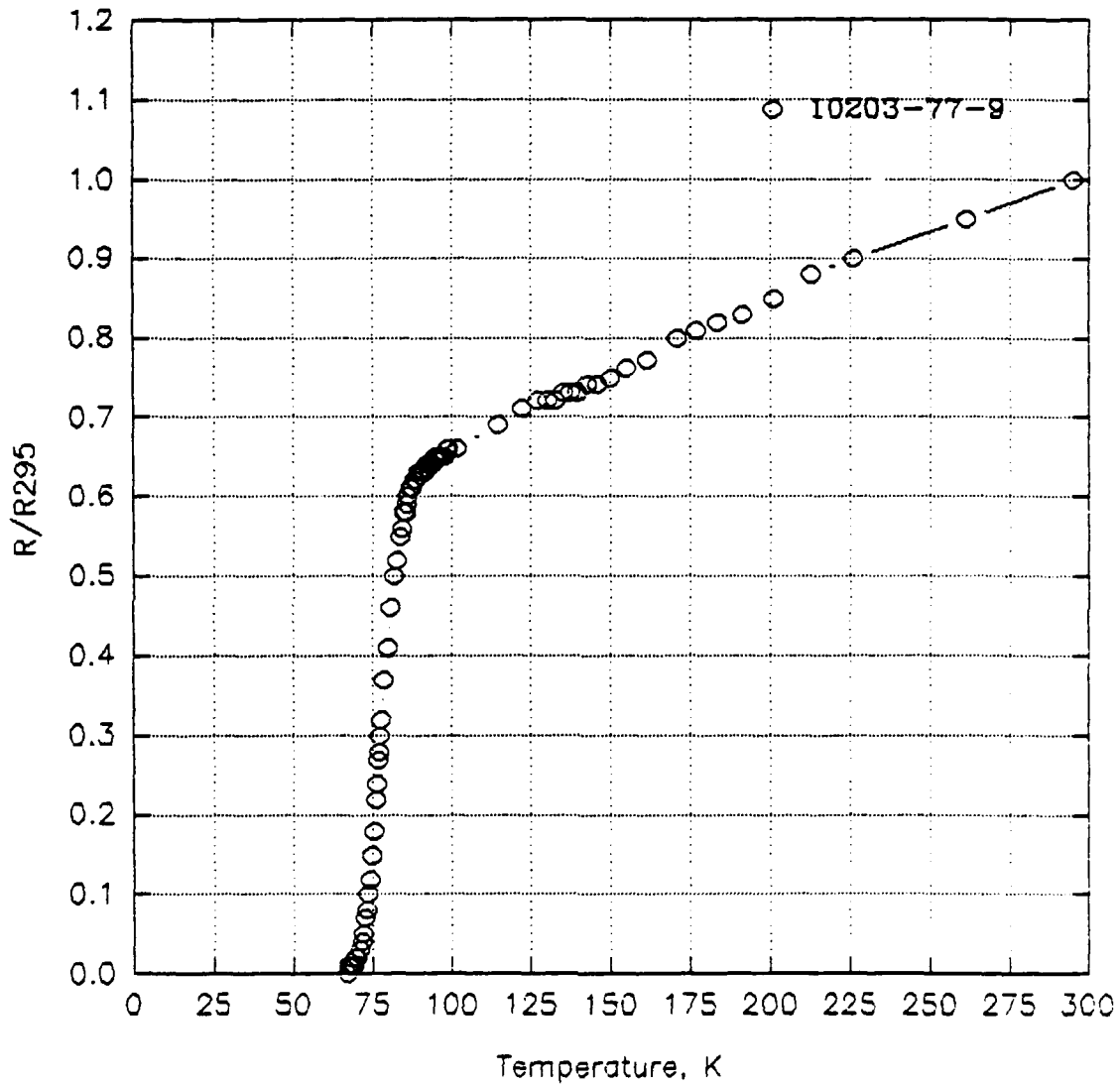
Fig. 3. Resistance vs temperature curve for the 123 film on SrTiO₃
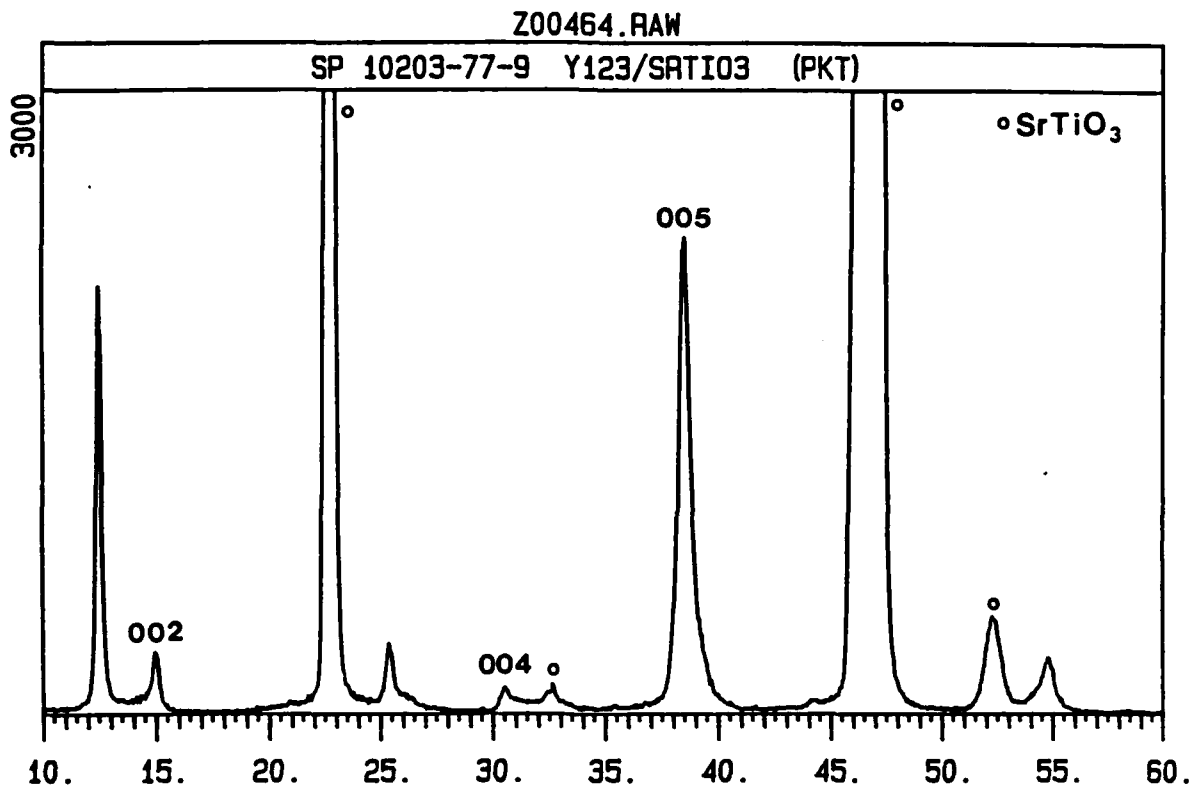
Z00464.RAW

SP 10203-77-9   Y123/SRTIO3   (PKT)

3000

∘SrTiO₃

005

002

004 ∘

∘

10.   15.   20.   25.   30.   35.   40.   45.   50.   55.   60.
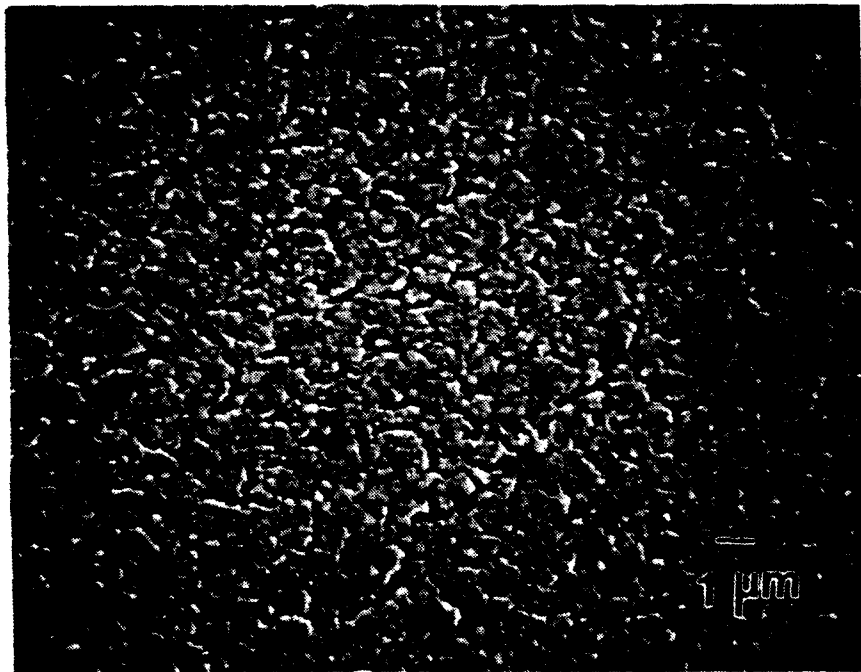
Fig. 4.   XRD pattern of 123 on SrTiO₃

2-11

Fig. 5. SEM photograph of 123 on SrTiO$_3$

complications in analysis, Ag was chosen as the substrate material for this study.

Figure 6 shows the film morphologies observed after heat treating to various temperatures and times. The SEM photographs show that full densification does not occur even at 920°C for 10 min. However, by holding at 920°C for 3 h, full densification was achieved. It is worth noting, however, that numerous microcracks occurred as a consequence of thermal expansion mismatch. It has been shown that finer grain size would minimize or eliminate the microcracking and that a heat treatment at 920°C for approximately 30 min will remedy the situation.

2.2.1. Grain Alignment

During the study to determine the right heat treatment condition, it was observed that a high degree of c-axis orientation was attained at elevated temperatures. As shown by the XRD patterns in Fig. 7, {001} peaks are enhanced when the films were heat treated beyond 920°C for 10 min. As observed in the SEM micrographs (Fig. 6), the degree of alignment improved with increasing isothermal holding time. For example, the ratio of (006) to (110) peaks was 12 for the sample heat treated for 30 min at 920°C, where as it was 200 for the sample held at the same temperature for 3 h.

Since it was difficult to measure the quality of the film on Ag by dc resistance, due to the exceptionally low resistivity of silver, dc susceptibility measurements were carried out at UCSD and the results are shown under electromagnetic property characterization.

2.2.2. Ag Substrate Effect on Alignment

In order to test whether grain growth of Ag was responsible for c-axis alignment, a pair of Ag substrates were prepared. One was heat treated in O_2 at 920° for 10 min and the other was left untreated. The
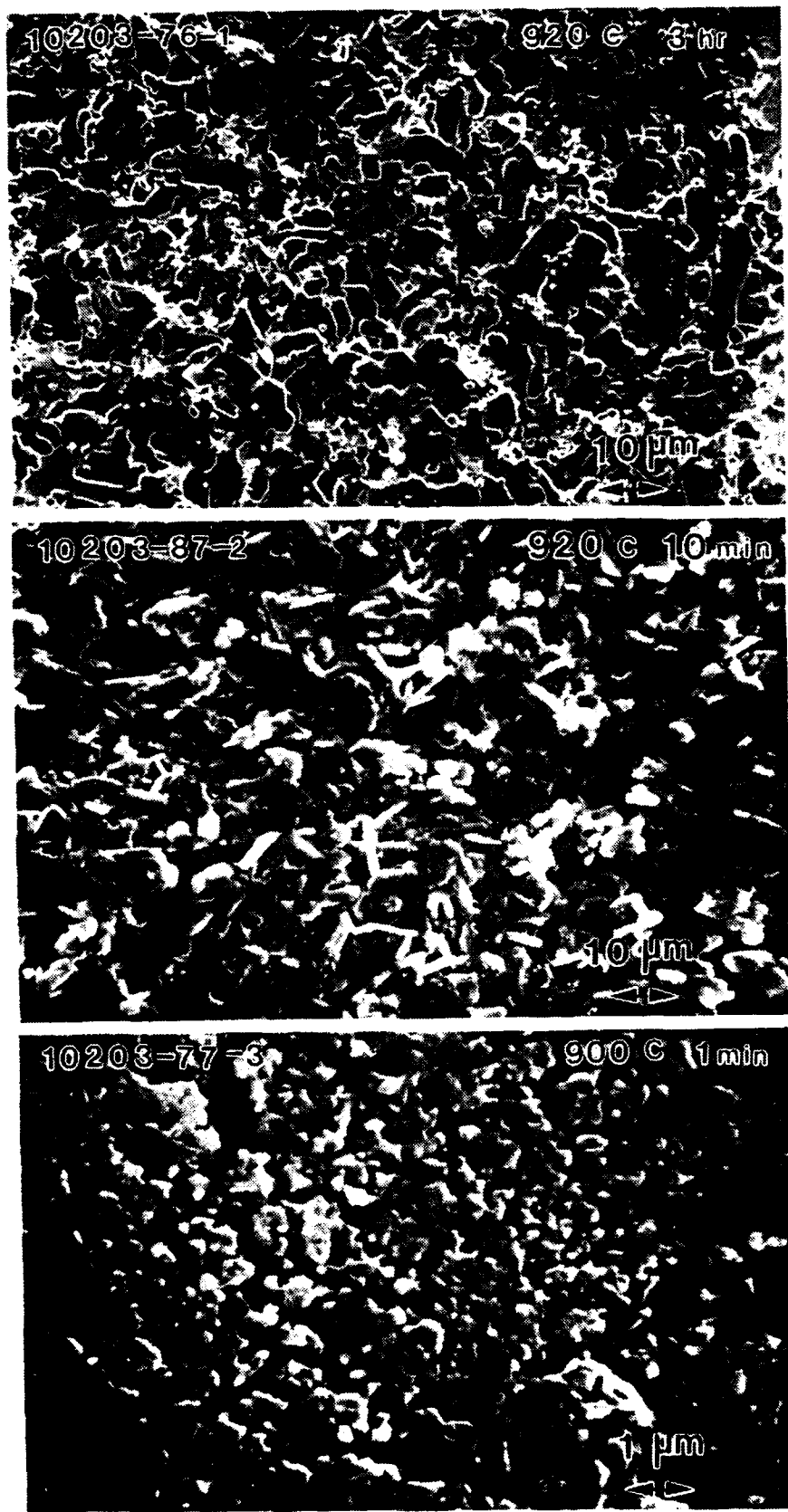
Fig. 6. SEM photographs of 123 film heat treated at the indicated temperatures and times
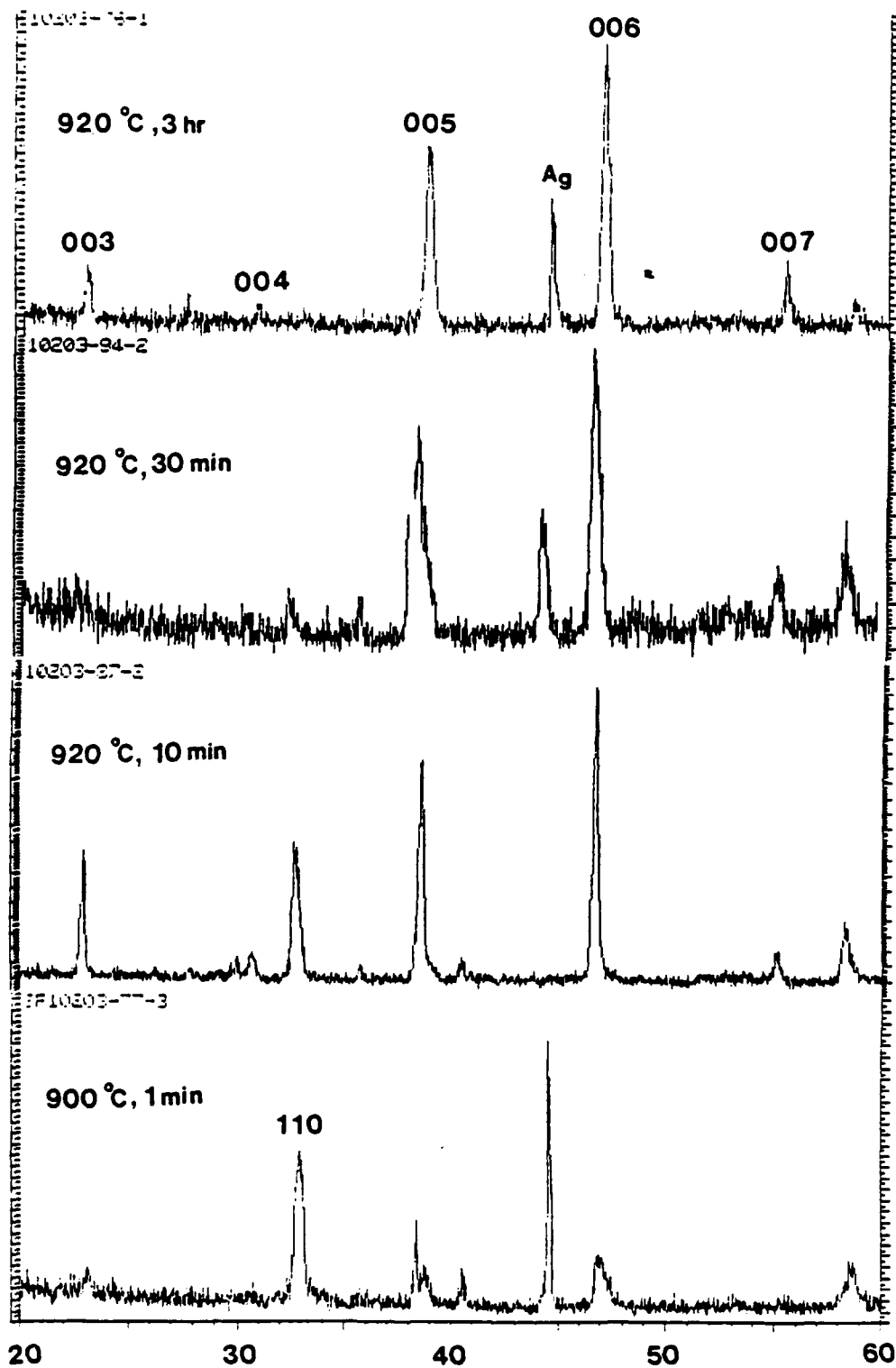
Fig. 7. XRD patterns of 123 films on Ag heat treated to indicated temperatures and times

heat treatment caused the Ag grains to grow to a size approximately 1 mm in diameter. The two substrates were dipped simultaneously and heat treated at 920°C for 30 min in flowing O_2.

The XRD results (Fig. 7) show the film on heat treated Ag was aligned twice as much as the one without the heat treatment. This suggests heteroepitaxial growth and needs further investigation for confirmation.

2.2.3. 123 Film on YSZP

As stated previously, 123 is known to react with YSZ at temperatures beyond 900°. This fact, combined with the information we have gained from the Ag work, that is a heat treatment at 920°C for greater than 10 min is necessary for full densification, it became apparent that a minimum 123 layer thickness is required to compensate for the inherent reaction that occurs with YSZP substrate.

For this study polished YSZP substrates were dipped 9, 12, and 20 times in air, pyrolyzed at 500°C and heat treated at 920°C for 10 min in O_2. Figure 8 shows the standard 4 point probe resistance curves obtained from the study. It is clear that with increasing thickness, the transition width sharpened dramatically. It appears that the film needs to be dipped at least 20 times, which corresponds to approximately 2 micrometers in thickness.

Since 20 dips are extremely time consuming and more importantly, often linked with surface irregularities, a feature intolerable in a high Q cavity, a new solvent was employed. By using normal hexane, C_6H_{12}, instead of toluene, the resin could be concentrated to as high as 50 w/o without causing precipitation. As a reminder, the highest solid concentration the toluene system would allow, without causing precipitation, was approximately 30 w/o. With the new sol, only 5 to 6 dips were required to build up the same coating thickness.
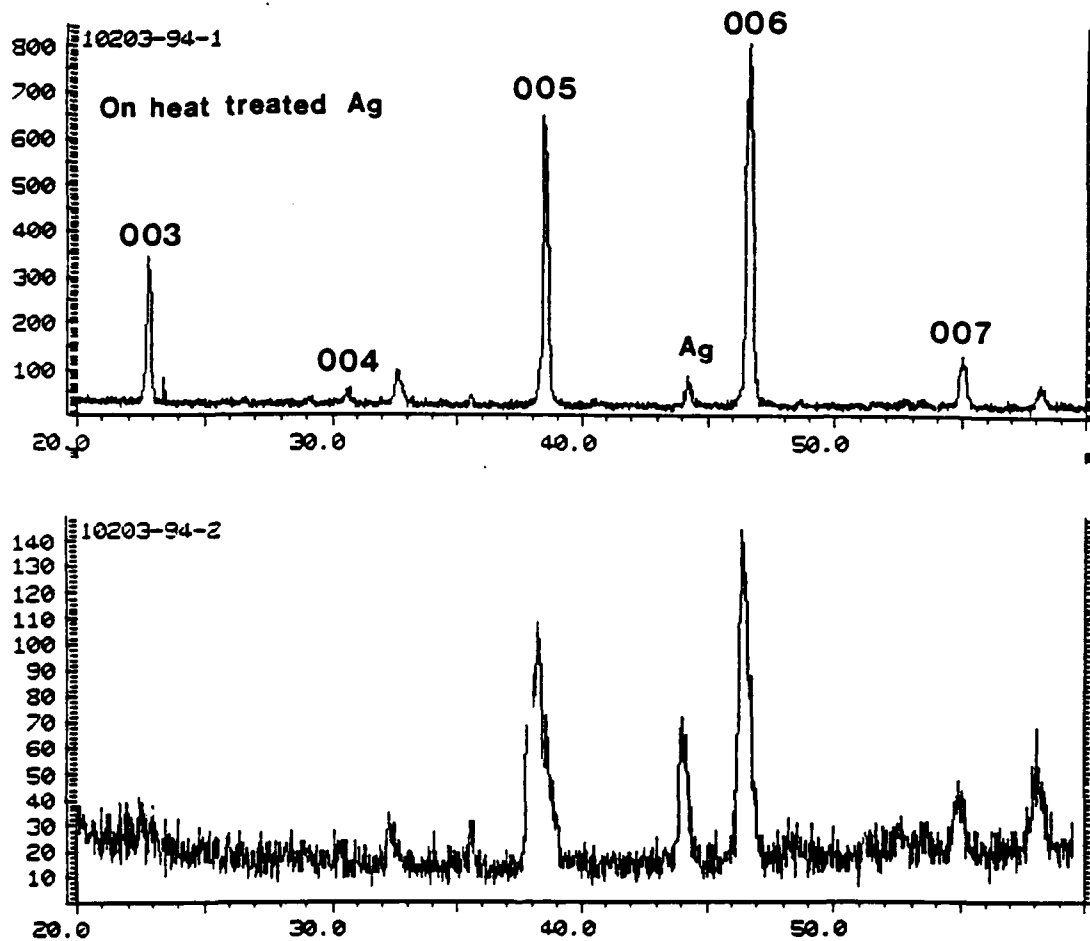
Fig. 8. XRD patterns of the 123 films prepared on heat treated (upper figure) and untreated (lower figure) Ag substrates
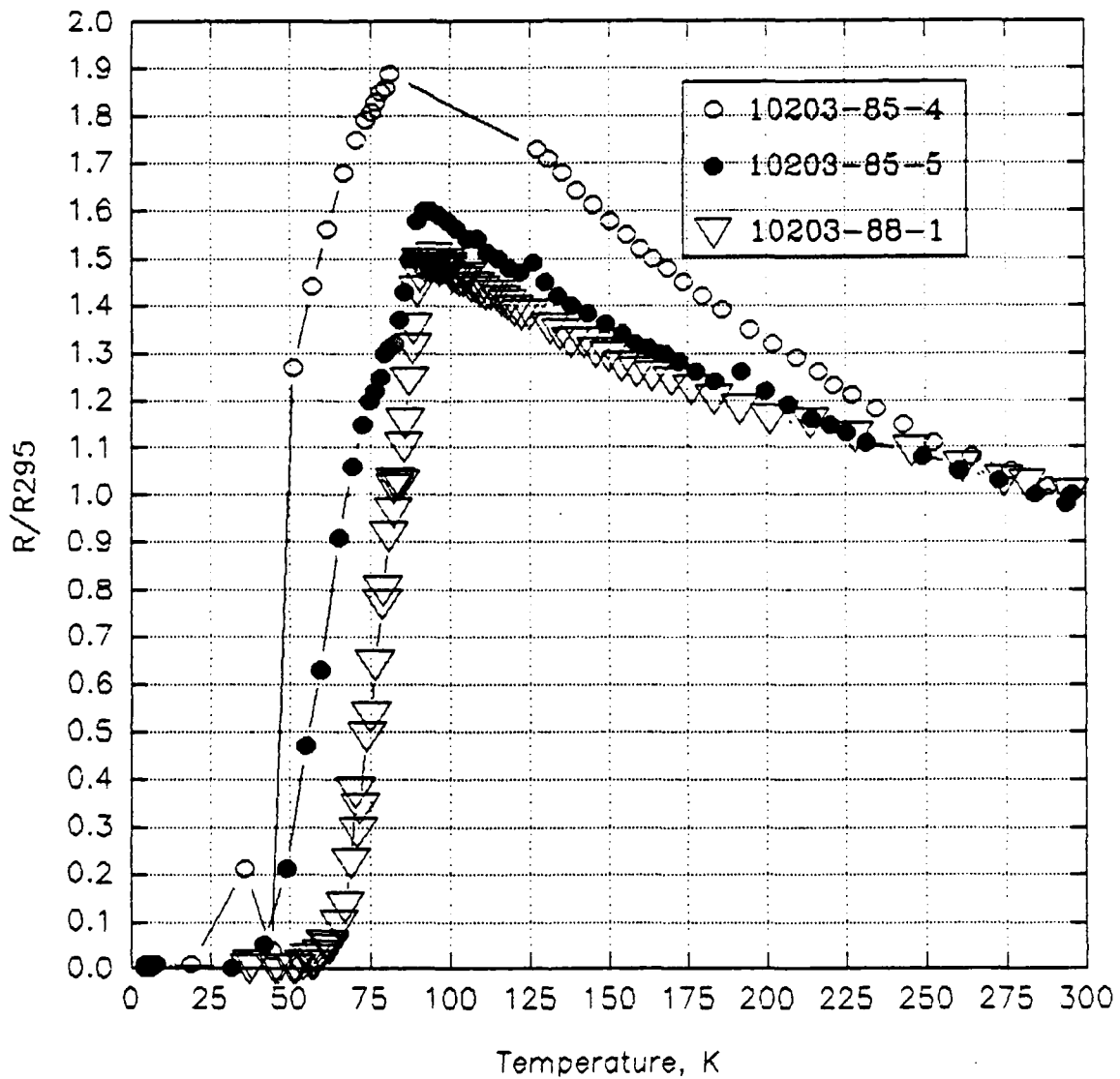
2-17

Fig. 9. Resistance vs temperature curves for 123 films on YSZP. The open circles represent 9 dips, closed circles 12 dips, and inverted triangles 20 dips.

2.3. PRELIMINARY 123 COATED CAVITY

Since promising results were obtained on Ag, a silver cavity cylinder and a disc were machined, cleaned, and coated with a freshly prepared sol. They were subsequently fired at 920°C for 30 min and annealed at 500°C for 12 h. Figure 10 shows that smooth coatings were obtained and their superconducting properties measurements are in progress.

2.4. 123 FILM FLUX PINNING

Lanthanum aluminate is currently being considered as a flux pinning additive for 123 fibers and films as well as diffusion barrier layer on ceramic substrates. We are developing methods of adding $LaAlO_3$ to the solutions from which films are formed.

2.4.1. Sol-Gel $LaAlO_3$

Lanthanum isopropoxide was prepared as described in the literature (Ref. 5). Lanthanum tri-2-(2-ethoxyethoxy)ethoxide was prepared by alcohol exchange with lanthanum isopropoxide. A solution containing 3.85 wt % equivalent $LaAlO_3$ was prepared from equal molar amounts of aluminum sec-butoxide (Aldrich chemical) and the above lanthanum alkoxide in 2-(2-ethoxyethoxy)ethanol. This solution was hydrolyzed at 56°C with 1 mole of water per mole of metal. A gel formed within 5 min after the water addition. With addition of enough solvent to give 1.95 wt % equivalent $LaAlO_3$, the gel could be liquefied by vigorous stirring. The solvent was then removed under vacuum at 55°C over 3 days.

Thermogravimetric analysis of the precursor powder produced as described above showed that the powder loses weight in oxygen until about 825°C. Furthermore, X-ray diffraction of the powder after annealing at 900°C for 10 min (Fig. 11) shows the pattern characteristic of
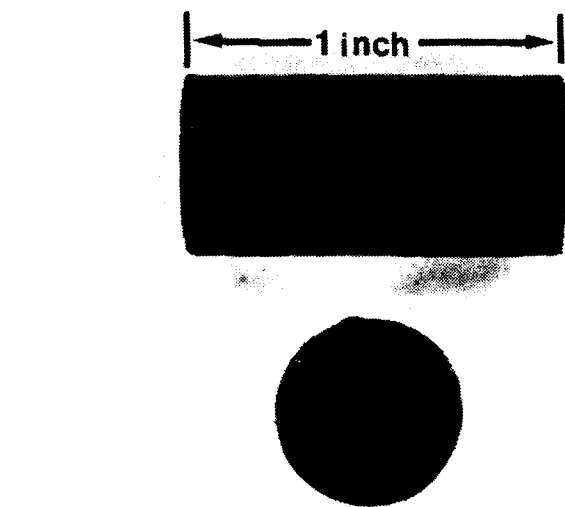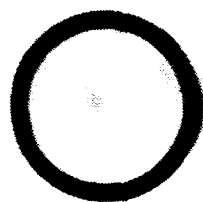
Fig. 10. 123 coatings on an Ag cylinder and a disc. The bottom photograph is the top view of the cylinder

Fig. 11. X-ray diffraction pattern for the composition La_2O_3:Al_2O_3 = 1:1 after heat treatment at 900°C for 10 min

LaAlO$_3$. Previous syntheses using the aluminum and lanthanum isoprop-oxides produced a white precursor powder which required heating to 1000°C for 30 min in order to form LaAlO$_3$.

2.4.2. 123 Solution Coated Ceramic Fibers
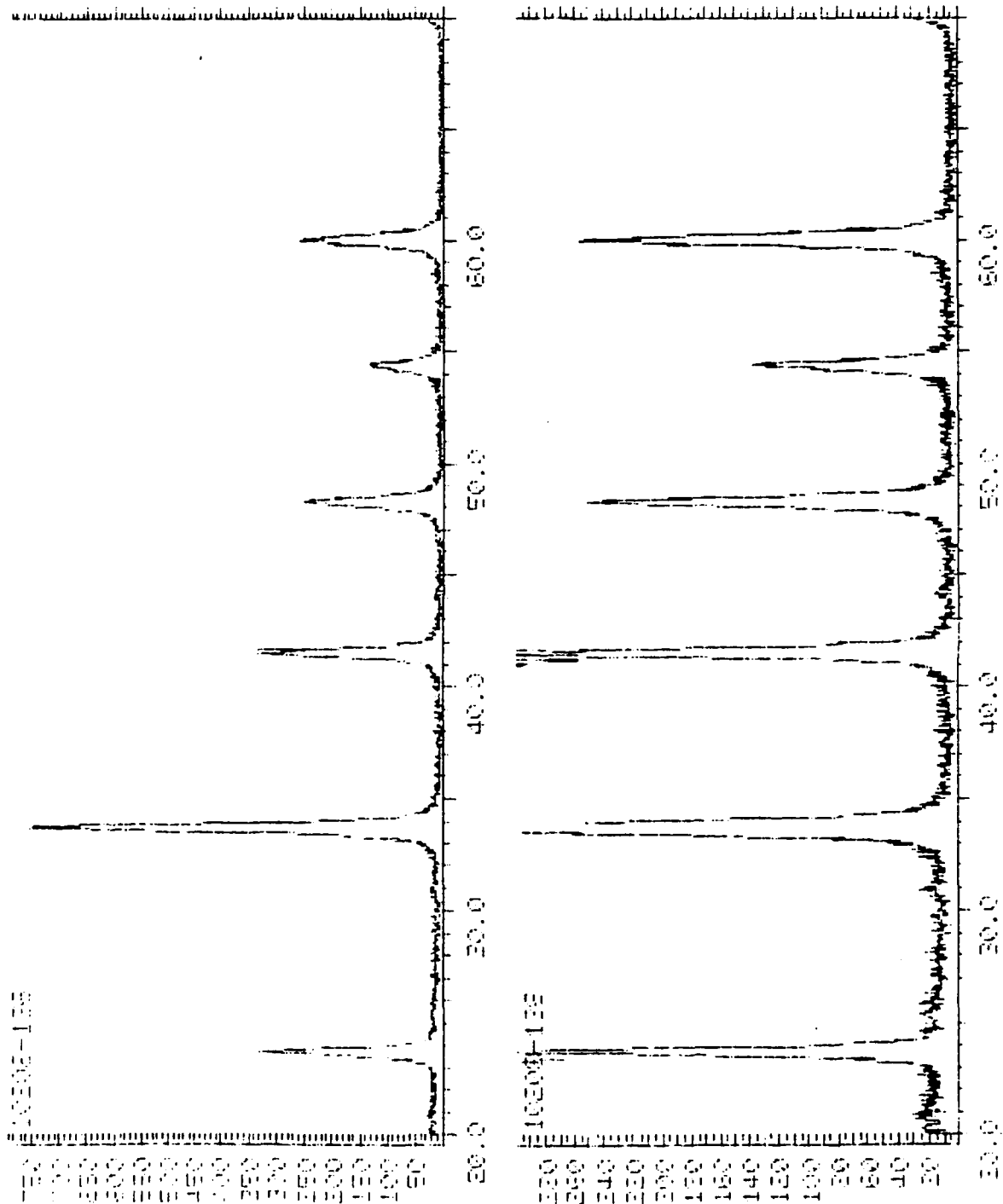
Two sol-gel derived barrier layer coatings, one with Y$_2$O$_3$ and another with LaAlO$_3$, on alumina substrates were made. EDAX analysis of the coating indicated that Y$_2$O$_3$ coating was thicker than the LaAlO$_3$ coating, Figs. 12a and 12b. The coated alumina substrates were then coated, using the automatic dip coater, with approximately 20 wt % 123 resin precursor in toluene and isopropanol solution. The processing conditions used for both barrier layer coatings and 123 solution coated samples are summarized in Table 3. The samples were then fired simul-taneously in a tube furnace to 825°C at a rate of 8°C/min with no hold time at temperature and cooled to 400°C at a rate of 10°C/min and finally furnace cooled to room temperature in flowing oxygen.

The resistivity measurements of the coated samples, Fig. 13, show that LaAlO$_3$ coated sample has T$_c$ onset at ~88 K and zero resistance at 21 K as compared to Y$_2$O$_3$ coated sample which exhibit T$_c$ onset at 86 K and zero resistance at ~7 K. Even though the Y$_2$O$_3$ barrier layer was thicker than the LaAlO$_3$ coating, the latter coating is seen to be more effective diffusion barrier layer for 123 material.

In order to develop a thicker LaAlO$_3$ coating, a much higher con-centration La/Al alkoxide solution was prepared. In addition, for the demonstration feasibility study of ceramic fiber coating, due to han-dling difficulty of PRD-166 fibers, much stronger and larger diameter (150 μm) sapphire fibers were used instead. Sapphire fibers were man-ually dipped 3 or 4 times in the glove box followed by hydrolysis in air outside the glove box. Three sets of fibers were coated a total of 10 times using different solution concentrations as summarized in Table 4.

23-MAR-90 14:24:27 SUPER QUANT
RATE= 1648CPS   TIME= 238LSEC
FS=   2986/   2986 PRST=   OFF
A = 10377-50-02

AlKα

LaLα

2.00   4.00   6.00   8.00
222CNT   1.91KEV   10eV/ch A EDAX
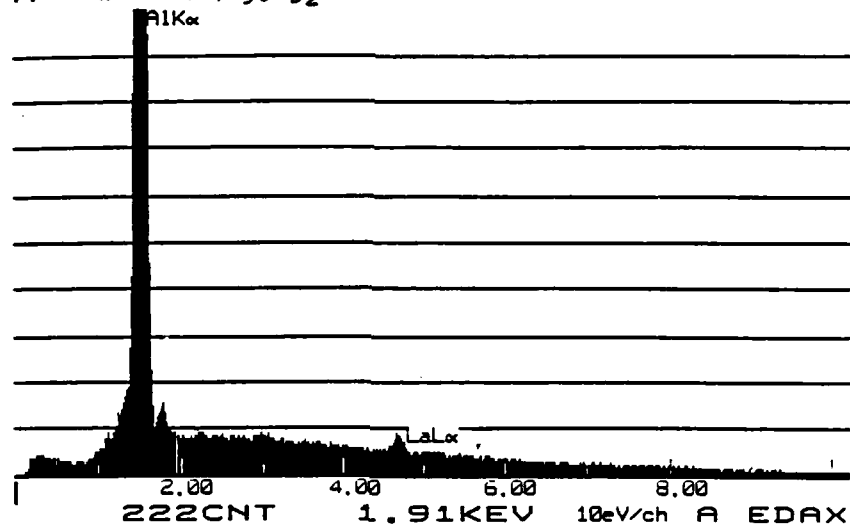
05-APR-90 10:06:57 EDAX STORE
RATE=   2CPS   TIME= 284LSEC
FS=   455CNT   PRST=   OFF
A =

ZrLα

LaLα

2.00   4.00   6.00   8.00
54CNT   4.63KEV   10eV/ch A EDAX
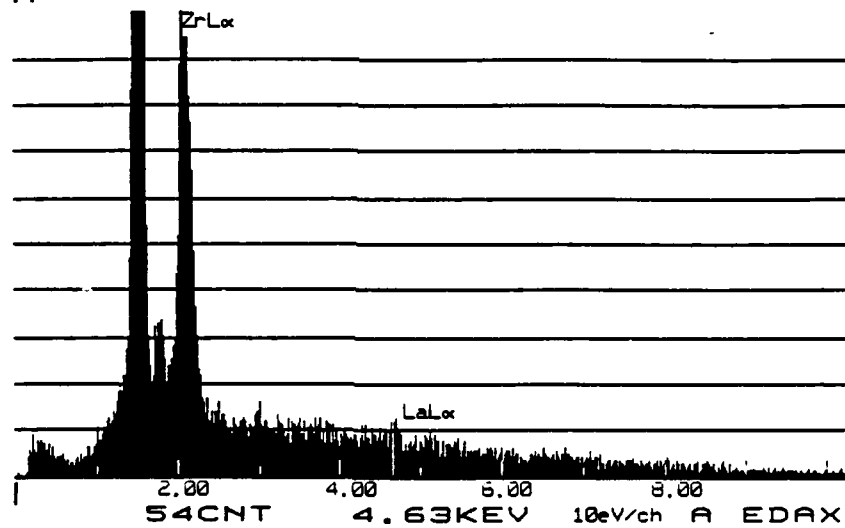
Fig. 12. EDAX results of LaAlO$_3$ barrier layer coating (a) on alumina
          substrate after dipping 5 times in 0.0154 M solution; (b) on
          PRD-166 fibers after dipping 20 times in 0.0154 M solution

TABLE 3
COATING CONDITIONS FOR BARRIER LAYERS AND
123 PRECURSOR ON ALUMINA SUBSTRATES

Sample No.	10377-47-01	10377-50-02
Barrier layer	Y_2O_3	$LaAlO_3$
Mechanic	Dip coater	Dip coater
Dipping cycle	10 times	5 times
Concentration	0.017 Molar	0.0154 Molar
Atmosphere	N_2	N_2
Heating schedule	RT -- 900°C -- 900°C -- RT	RT -- 1000°C -- 1000°C -- RT
Mechanical	Dip coater	Dip coater
Dipping cycle	2 times	2 times
Concentration	~20 wt % 123 solution	~20 wt % 123 solution
Atmosphere	O_2	O_2
Heating between dipping cycle	500°C/10 sec	500°C/10 sec

Fig. 13. Resistivity measurements of two 123 solution coated alumina substrates

TABLE 4
COATING CONDITIONS FOR SAPPHIRE FIBERS IN
La/Al ISOPROPOXIDES SOLUTIONS

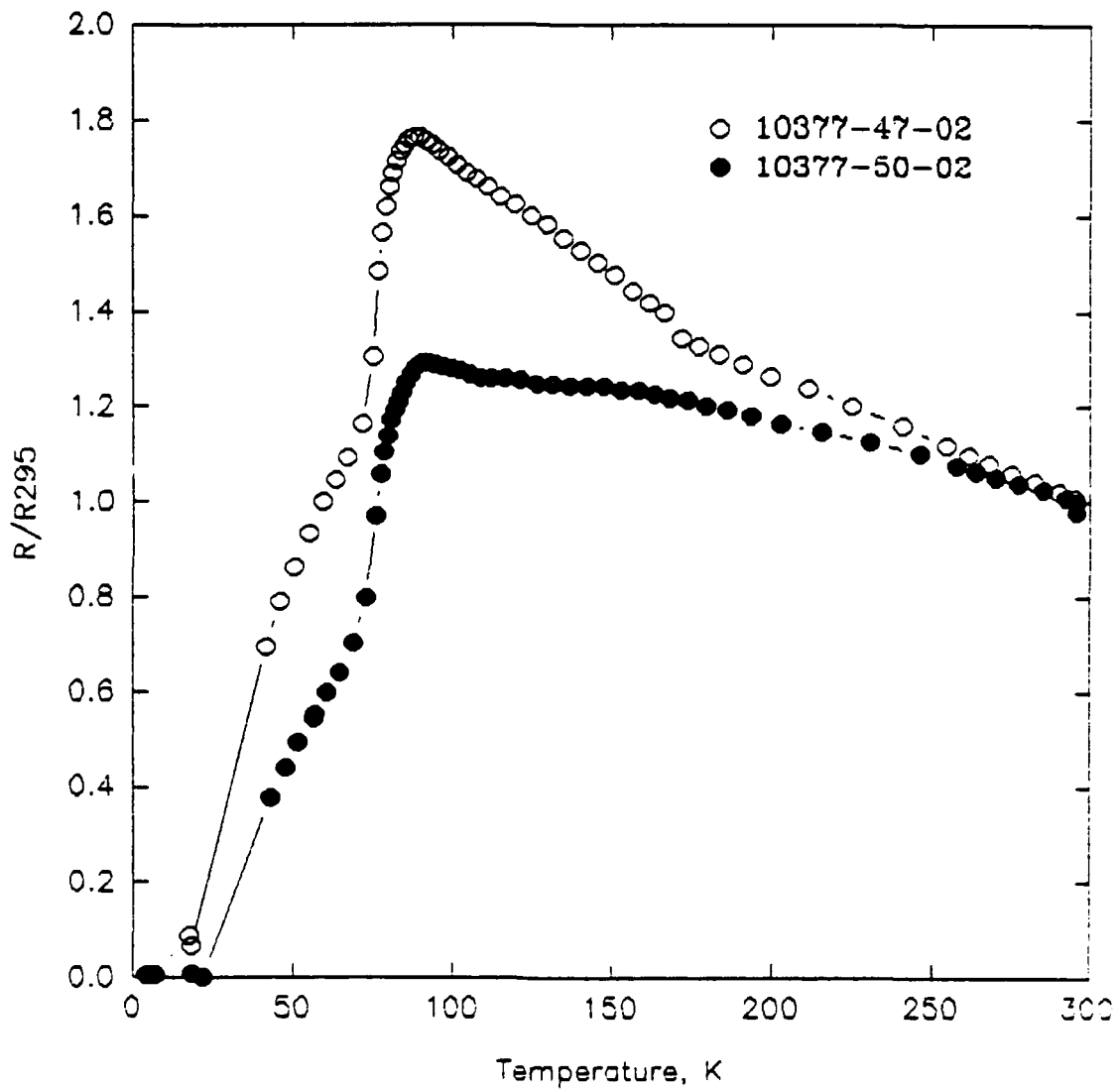| Sample No.	Concentration	Dipping Cycles
10377-59-01	0.140 M	10 times/manual
10377-59-02	0.093 M	10 times/manual
10377-59-03	0.047 M	10 times/manual

They were subsequently fired together in air with the following heating schedule:

$$RT \xrightarrow{5°C/min} 1000°C \xrightarrow{5°C/min} RT$$

To determine the coating thickness of the fiber sample the counting rate and time were kept constant while using EDAX for each set of four fibers. The amount of La element shows the highest count on the fibers coated with the most concentrated La/Al isopropoxides, Fig. 14. However, samples dipped 10 times in 0.140 molar and 0.047 molar solutions displayed serious cracking problems as shown in Figs. 15a and 15b. However, promising microstructure was observed in samples dipped 10 times in 0.093 molar solution as shown in Fig. 15c. Therefore, additional sapphire fibers will be dipped in 0.093 molar solution while experimenting with a different number of dipping cycles and firing conditions.

Because the molar ratio of Al and La couldn't be accurately determined on the coated sapphire fiber, 2 YSZP substrates were coated as reference material with 0.140 M solution ten times and three times, respectively.

The EDAX results, although semi-quantitative, of the fired substrates show that the molar ratio is approximately one as listed in Table 5.

2.5. SCALE-UP COMPOSITION STUDY OF 123 PRECURSOR SOLUTION

Large batches of yttrium and barium isopropoxides and copper hexanoic acid were prepared and the solution concentrations, in terms of g/mole, were determined by EDTA titration. A small batch of 123 solution was prepared and mixed in exact proportion to give oxide molar ratio of Y1.00 Ba2.00 Cu3.00. It was then followed by a series of small batches prepared in the designated proportion, based on the weight of each constituent in the first batch, to give the desired oxide molar
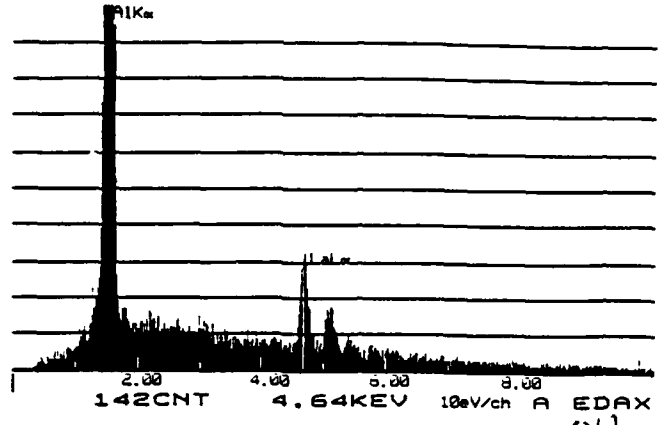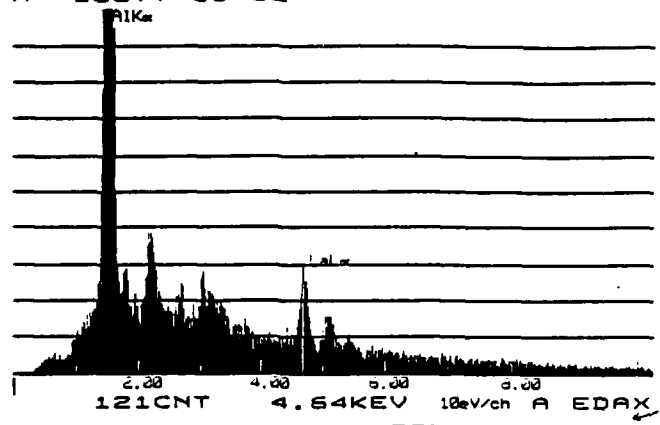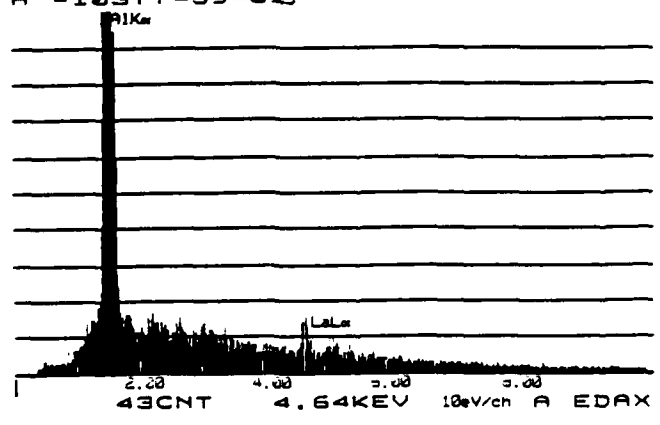
Fig. 14. The EDAX results of coated sapphire fibers in La/Al
isopropoxides solutions. (a) In 0.140 M/10 times,
(b) in 0.093 M/10 times, (c) in 0.043 M/10 times

2-28
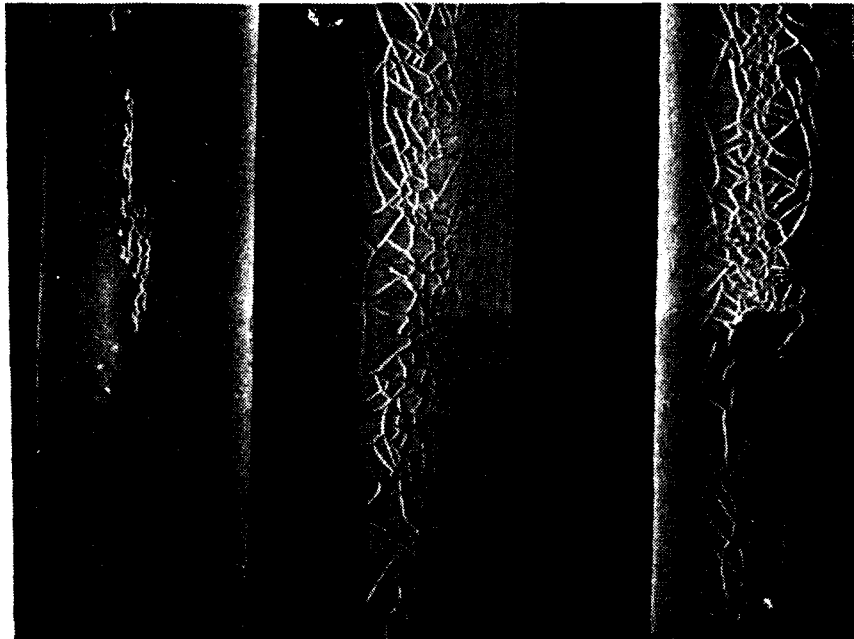
200x   4a

200x   4b

Fig. 15.   SEM of the coated sapphire fibers in La/Al isopropoxides
           solutions.   (a) In 0.140 M/10 times, (b) in 0.093 M/10 times,
           (c) in 0.047 M/10 times (sheet 1 of 2)
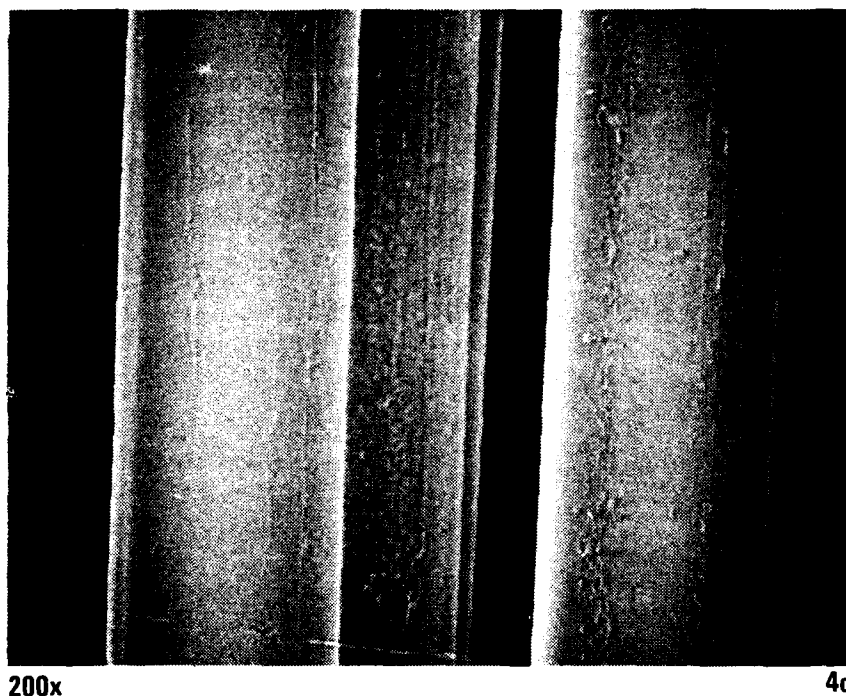
2-29

200x 4c

Fig. 15. SEM of the coated sapphire fibers in La/Al isopropoxides
solutions. (a) In 0.140 M/10 times, (b) in 0.093 M/10 times,
(c) in 0.047 M/10 times (sheet 2 of 2)

2-30

TABLE 5
EDAX RESULTS OF COATED YSZP SUBSTRATES IN 0.140 M
La/Al ISOPROPOXIDES SOLUTION

Sample No.	Dipping Cycle	Al Element wt %	La Element wt %	Thickness 1 μm
10377-59-Zr03	3 times	54.23	45.77	1
10377-59-Zr04	10 times	51.87	48.13	0.4

ratio. Thin fibers were then drawn manually from the precursor resin and fired in O_2 at 900°C for 8 h.

From the DTA results obtained so far for all the batches, we have narrowed down the composition region where the precursor produces almost no low melting phases, Fig. 16. However, a few more batches with these composition ratios have to be prepared in larger batches to verify its reproducibility. Once it's confirmed on the exact composition ratio and reproducibility, the remaining stock solutions will be used up to prepare a large preceramic resin batch for the remainder of the program for process specification.

2.6. FIBER PROCESSING

2.6.1. Extrusion of 123 Filaments/Rods

Since the fibers hand-drawn or spun from all sol-gel preceramic resin undergoes a large shrinkage, 50% or more, during organic pyrolysis and sintering which often results in cracking and weak fibers; 123 powders were used as filler material with the preceramic resin to reduce the shrinkage during firing.

Two kinds of 123 powder were utilized: one commercially available powder from Rhone-Poulenc and another experimental laboratory powder from the Argonne National Laboratory. The DTA and XRD have been performed to characterize the as-received and after-calcined 123 powders. Some 211 phases were detected in the XRD patterns of both as-received powders but they disappeared after being calcined at 900°C for 8 h in O_2. However, for both powders, the DTA results did not show much difference between the as-received and after calcination, namely the powders contained some impurity phases and melting occurred above ~920°C.
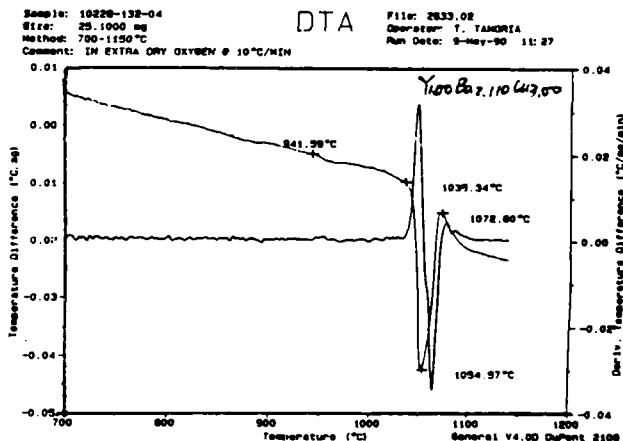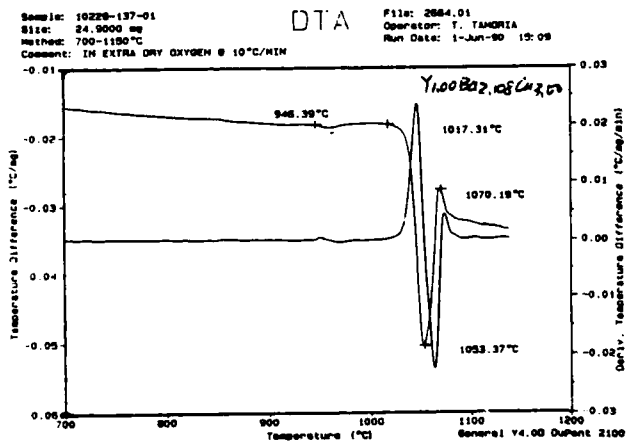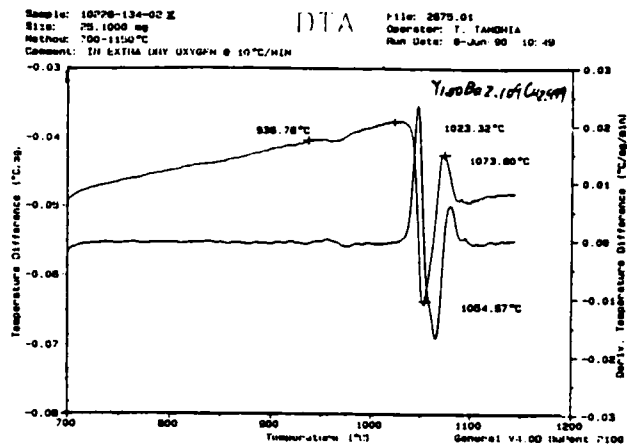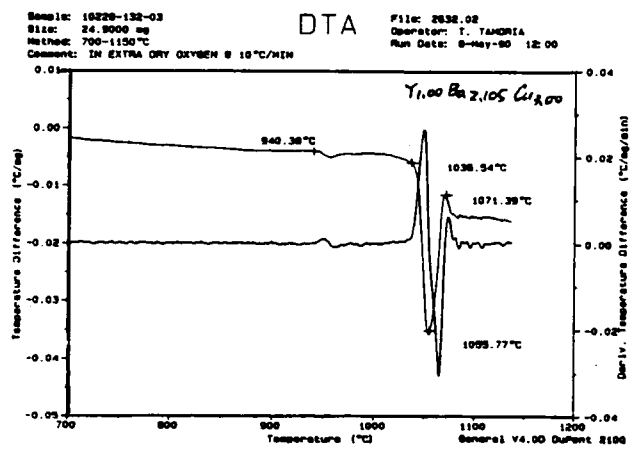
Fig. 16. DTA results of some of the prepared batches which have small or no low melting phases

A summary of the extruded filaments and their Jc measurements are tabulated in Table 6. Even though the weight percent of each constituent was approximately the same for batches using either Rhone-Poulenc 123 powder or Argon 123 powder, a rheological behavior difference was observed during filaments extrusion. The batch consisting of Argon 123 powder exhibited good solvent retention capability and long filaments of two different diameters were successfully extruded. On the other hand, the solvent tended to be squeezed out from the Rhone-Poulenc batch which resulted in a continuous increase of extrusion pressure. The extruded filaments of larger diameter were very weak and often broke into smaller pieces while hanging to dry after extrusion.

2.7. IMPROVEMENT OF FIBER CURRENT DENSITY

In the previous report, sol-gel derived fibers of 123 with T_c of 90 to 91.5 K and ΔT = 1.5 to 2 K were reported. However, the current density of the fibers were only in the range of 50 to 200 A/cm^2. Therefore, during the past quarter, we have focused on improving the current density of these fibers.

The low current density in the fibers were believed to be due to undesirable microstructure, which includes cracking, large grain size, large size porosity, and second phases. The problem of axial cracking usually occurred during the low temperature (200° to 400°C) organic pyrolysis has been solved by using a stepwise heat treatment schedule as described previously. The curing pyrolysis schedule requires 3 days to allow the organic pyrolysis by-products to diffuse out from the interior of the fiber. At the present time, fibers without axial cracking are routinely obtained. While the improvement of the heat treatment schedule is still being investigated, mainly to shorten the heat treatment schedule, in order to streamline the processing time and to test heat treatment reliability, it is believed that the axial cracking was not the major cause of low current density.

TABLE 6
SUMMARY OF EXTRUDED 123 FILAMENTS/RODS

Sample No.	Firing Condition	Powder Used	Diameter	Jc Measurement
10377-01	920°C (24 h)/ 935°C (5 h)/ 400°C (24 h)	Rhone-Poulenc	0.045 in.	500 A/cm^2 at 77 K 2000 A/cm^2 at 50 K
10377-03	920°C (12 h)/ 400°C (24 h)	Rhone-Poulenc	0.3 mm	12.7 A/cm^2 at 77.6 K 800 A/cm^2 at 18.9 K
10377-03	920°C (36 h)/ 450°C (24 h)	Rhone-Poulenc	0.3 mm	~465 A/cm^2 at 77 K
10377-012	930°C (12 h)	Argon	0.3 mm	~350 A/cm^2 at 77 K

Examining the microstructure of the polished crossed sections of the fibers, we found that the grain size (randomly oriented) of the fibers were too big so that it is possible that the major part of the current flow in the fiber is limited by only a few number of big crystals of unfavorable orientation, Fig. 17. The large grain size in the fibers can be clearly seen by using a polarized optical microscopy [Fig. 18 (a), (b)]. The large grain size in the fiber was partially due to the prolonged time and higher temperature used in an attempt to densify the fiber and also due to very slightly off-stoichiometry from 123 composition in the fiber. The fibers made from the batch 10105-85 II having a finer grain size as compared to the fibers from batch 10105-91 was attributed to a very slight composition fluctuation noting that both are DTA pure. The smaller grain size of batch 10105-85 II is shown in Fig. 19(a). A significant amount of porosity was also observed indicating further densification would increase the current density [Fig. 19(b)].

The experimental results indicate that in order to improve current density of the 123 fibers, it is imperative to improve the microstructure of the fibers. In an attempt to do that, first the maximum sintering condition was adjusted from 950°C for 24 h to 915°C for 24 h to reduce the grain growth during sintering. The grain size became smaller with decreasing temperature as shown in Fig. 20(a). However, the density of the fibers decreased as more pores were observed [Fig. 20(b)]. With a smaller grain size however, the average current density of three different samples measured were increased to approximately 1000 A/cm^2 (944, 1100, and 1220 A/cm^2).

To enhance the densification, it was decided to add 3 wt % 0.4 μm in diameter silver powder to the resin. The uniform fine distribution of the silver particles in the spun fiber after organic removal can be clearly seen in Fig. 21. Different temperature-time schedules were used to study the effect of silver addition on the densification of the fibers. Figure 22 shows a decrease in the porosity with silver addition

(a)

50μm
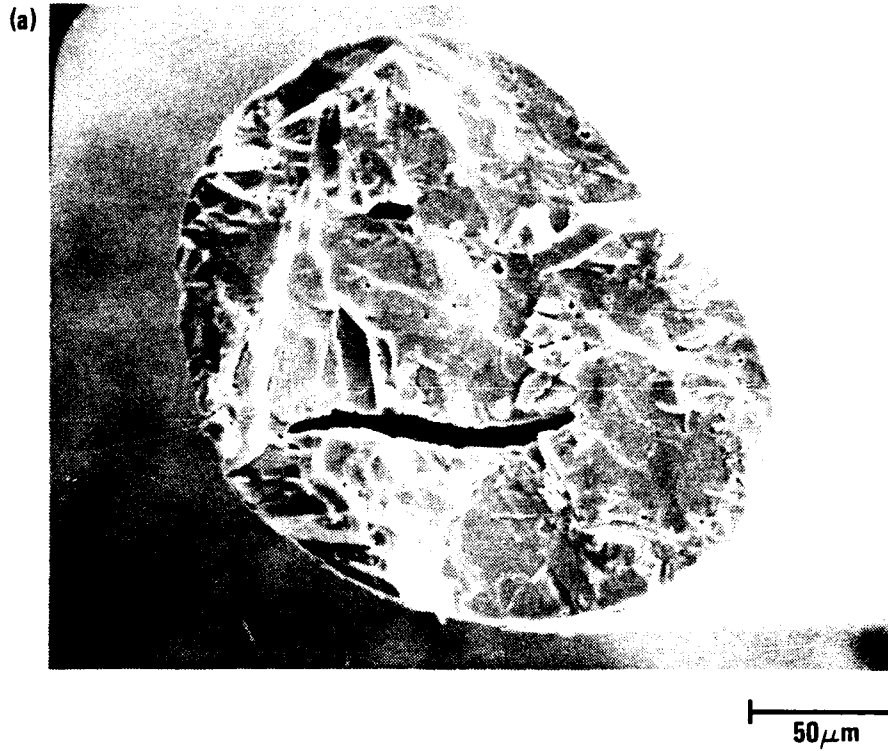
Fig. 17. Fracture surface of the fiber calcined at 935°C, 24 h, and
950°C, 5 h (Sample 10105-91 H51)

(a)

50μm

(b)
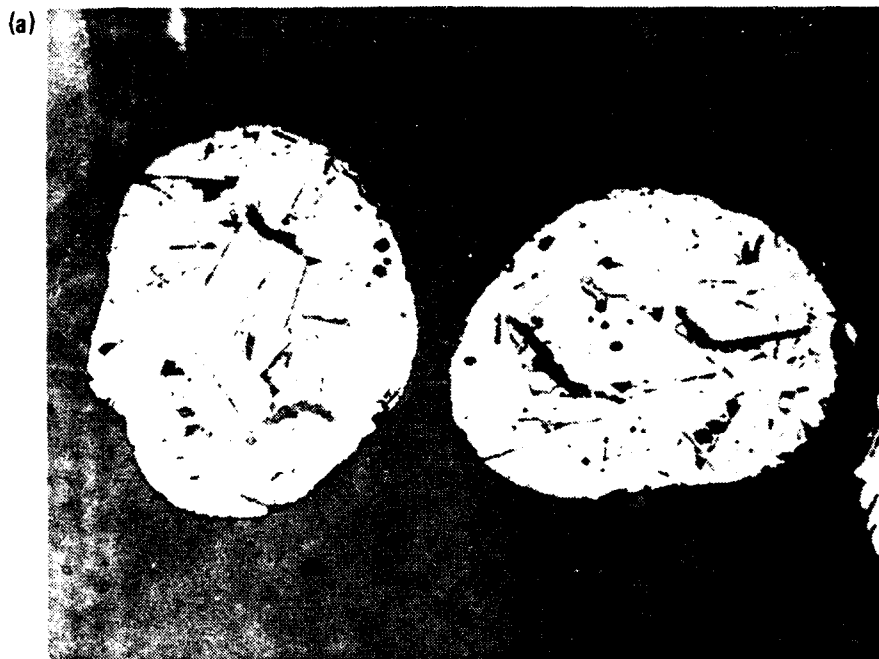
50μm

Fig. 18. (a) The polished cross section of fiber of Fig. 1 showing
large grain size and porosity (10105-91 H51; optical
microscope 300X); (b) under polarized light to clearly
reveal grain size (400X)
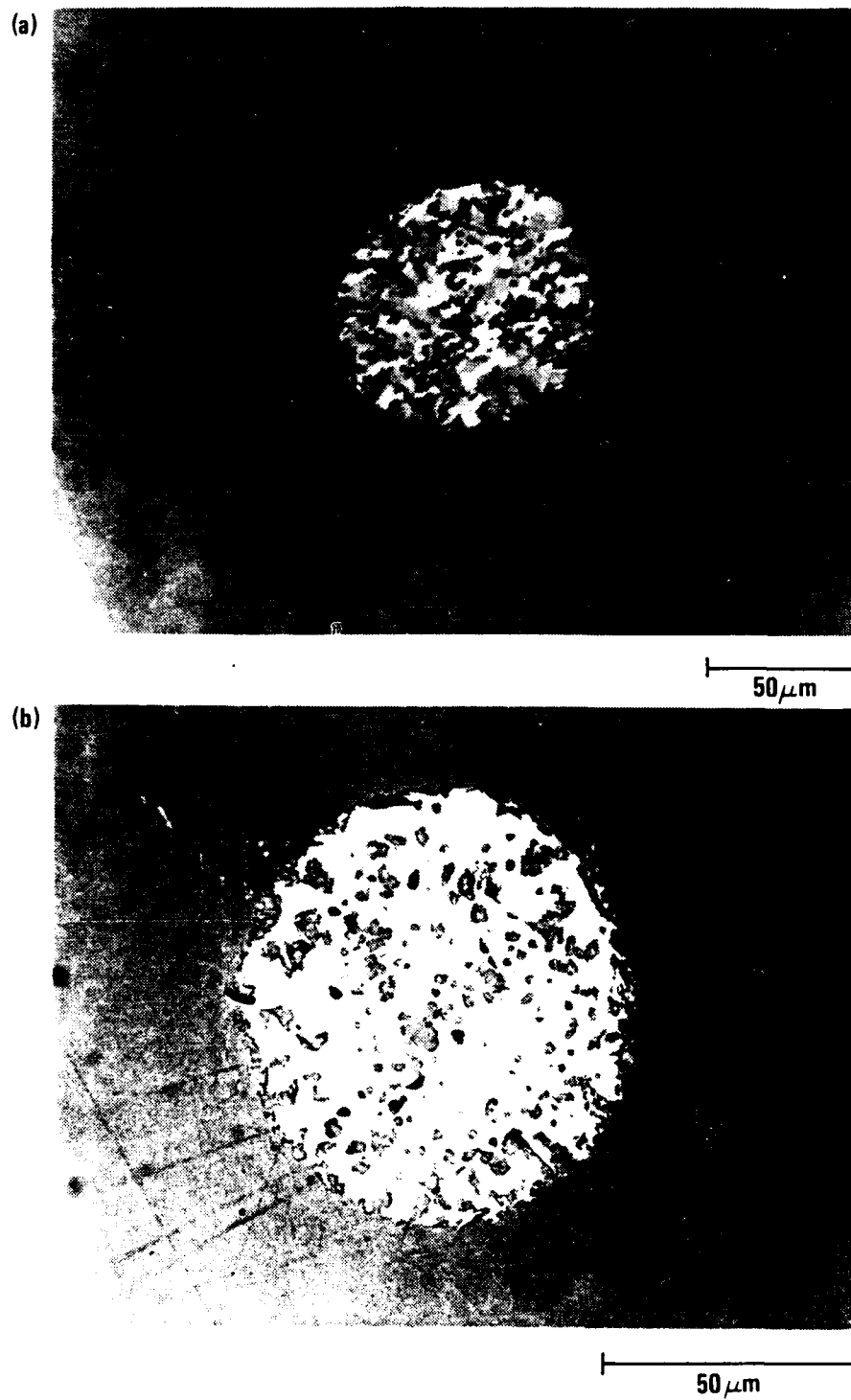
Fig. 19. (a) The optical micrograph of the polished cross section of
         fiber from batch 10105-85 II calcined at the same maximum
         temperature (935°C, 24 h, 950°C, 5 h) showing finer grain
         size under polarized light (400X); (b) unpolarized light to
         show porosity (700X)

(a)

(b)
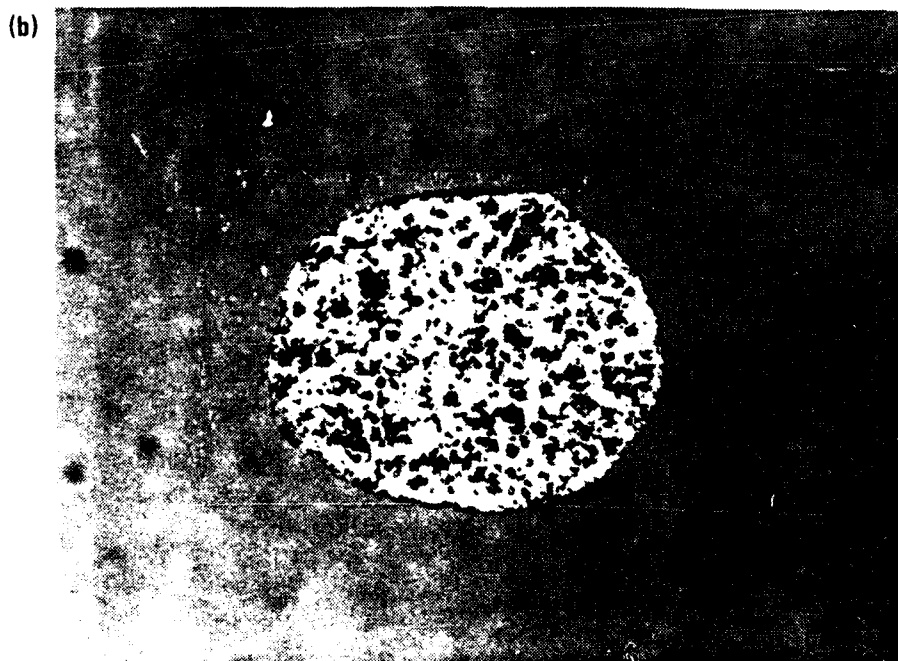
50 μm

Fig. 20. (a) The optical micrograph of the polished cross section of fiber calcined at 915°C, 24 h showing finer grain size (polarized light; 400X; Jc = 1100 A/cm^2); (b) unpolarized light to show a large amount of porosity (400X)
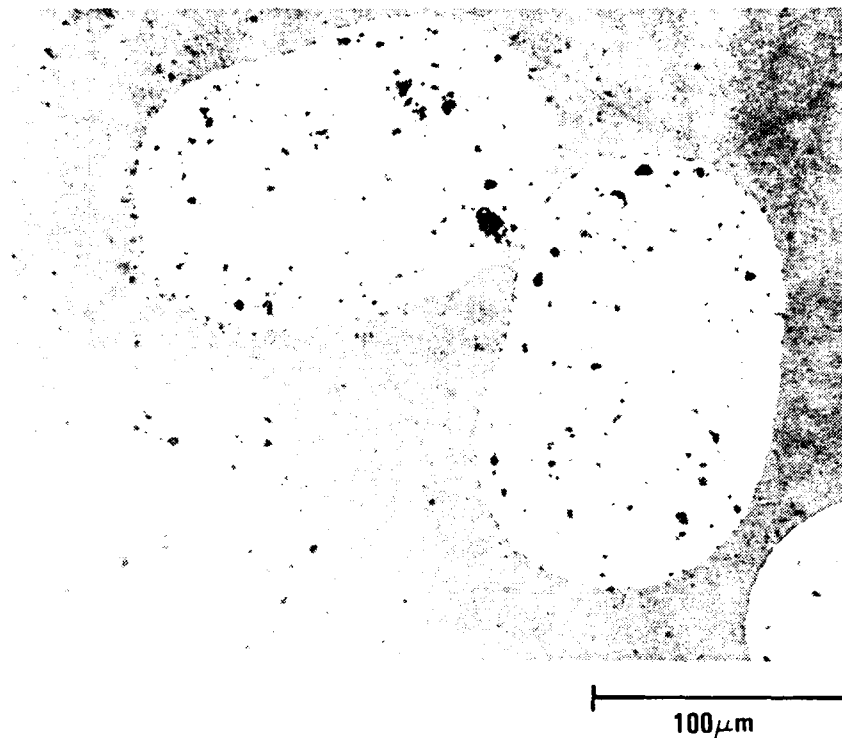
Fig. 21. The fiber with fine silver powder (3 wt % after calcination)
showing silver particles are well-distributed
(Sample 10105-85 II (Ag)-H66, 475°C max calcination, 300X)
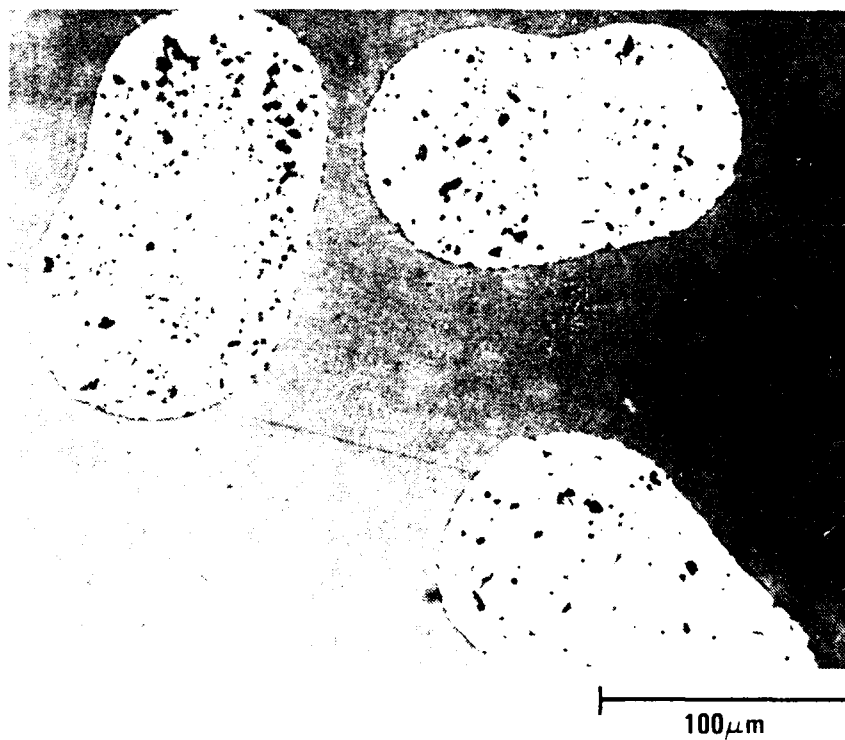
Fig. 22. The polished cross section of silver-added fiber calcined at
920°C, 18 h and 935°C 5 h showing decrease in porosity
(Sample 10105-85 II (Ag)-H72; 300X)

even though the maximum sintering temperature was decreased and the holding time was shortened [compared to Fig. 19(b)], the grain size was still considered too big. Figure 23 shows the cross section of the fiber with the sintering temperature lowered to 915°C for 12 h. The overall porosity increased but the pore sizes were smaller and more evenly distributed when compared with Fig. 19(b) and 20(b). Prolonging the sintering time at 915°C to 24 h, the porosity remained the same but the grain size remained small [Fig. 24(a) and (b)]. The current density of the fiber was improved and was in the range of 1400 ± 600 A/cm^2. A maximum current density of 2083 A/cm^2 was observed (77 K, zero field). It should be noted that further reduction in sintering temperature to 900°C for 24 h, decreased the current density of the fiber to 200 A/cm^2 with porosity remaining at the same level, Fig. 25. Detailed critical current density measurement on the fibers made are described under the electromagnetic properties characterization Section 3.1.

Based on the current density measurement, it is apparent that by improving the microstructure, it may be possible to double the fiber current density if fiber can be densified without excessive grain growth. In order to increase the current density further, the grain alignment of the fiber is the next essential step. The microstructure texturing of the fiber is in progress.

2.7.1. Reduction of the Fiber Shrinkage During Sintering

As mentioned previously, another obstacle for continuous processing of the sol-gel derived 123 fiber is that the fibers have a large dimensional shrinkage (approximately 50%) during sintering. In order to continuously sinter the fiber as it is spun from the spinneret, it is necessary to reduce the shrinkage. The shrinkage can be reduced by adding some fine Y123 powder to the resin. A 30 wt % of fine Y123 powder (provided by Argonne National Laboratory) was mixed with resin powder together with 3 wt % of fine silver powder. This addition of

50μm

Fig. 23. Optical micrograph of the polished cross section of the silver-added fiber calcined 915°C, 12 h showing porosity (Sample 10105-85 II(AG) H77,78; 400 X)

(a)

50μm

(b)

50μm
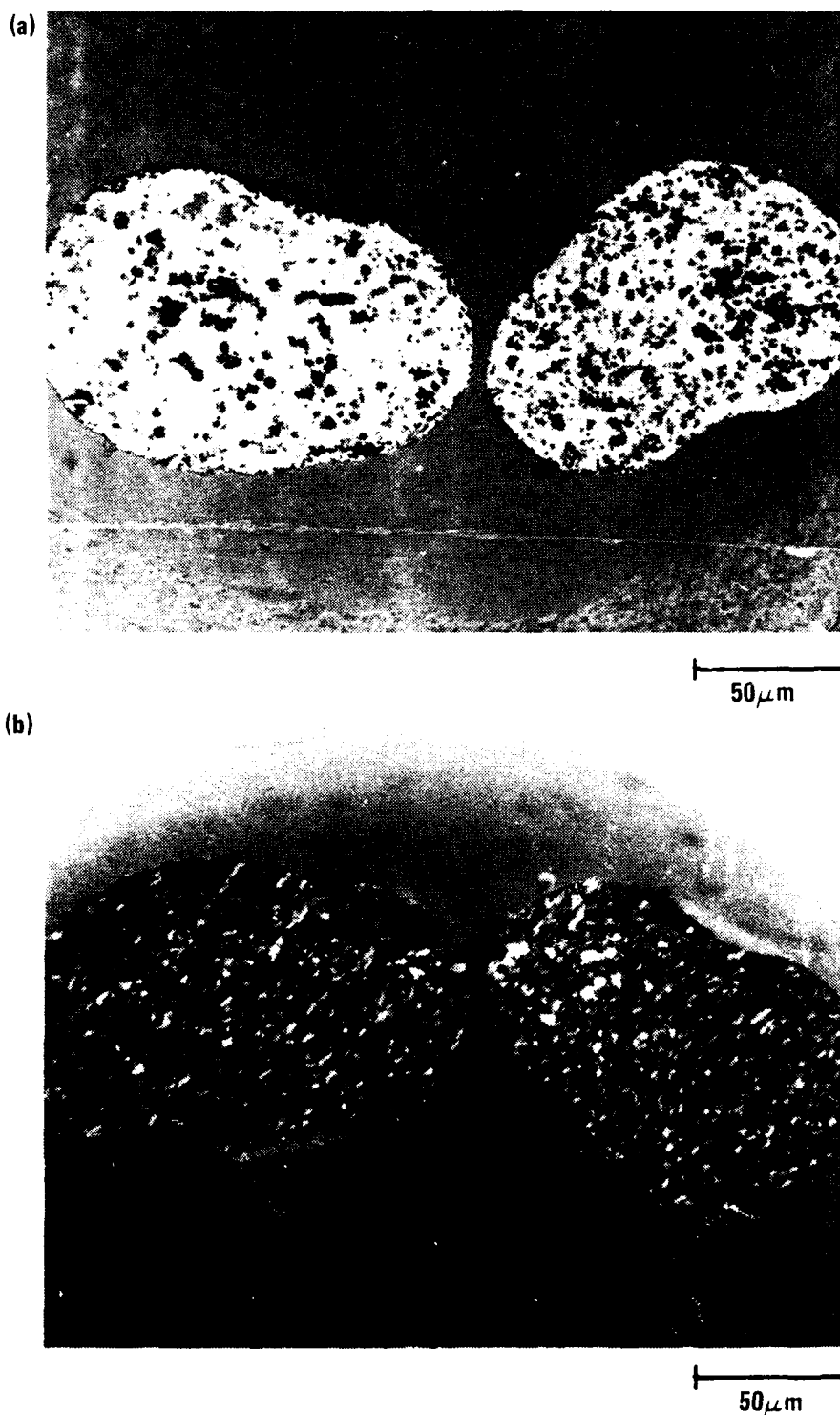
Fig. 24. (a) The polished cross section of fiber calcined at 915°C, 24 h showing porosity (Sample 10105-85 II(Ag) H70,75,57; 400X); (b) under polarized light to clearly reveal fine grain size (400X; J_c = 1000 to 2100 A/cm^2)
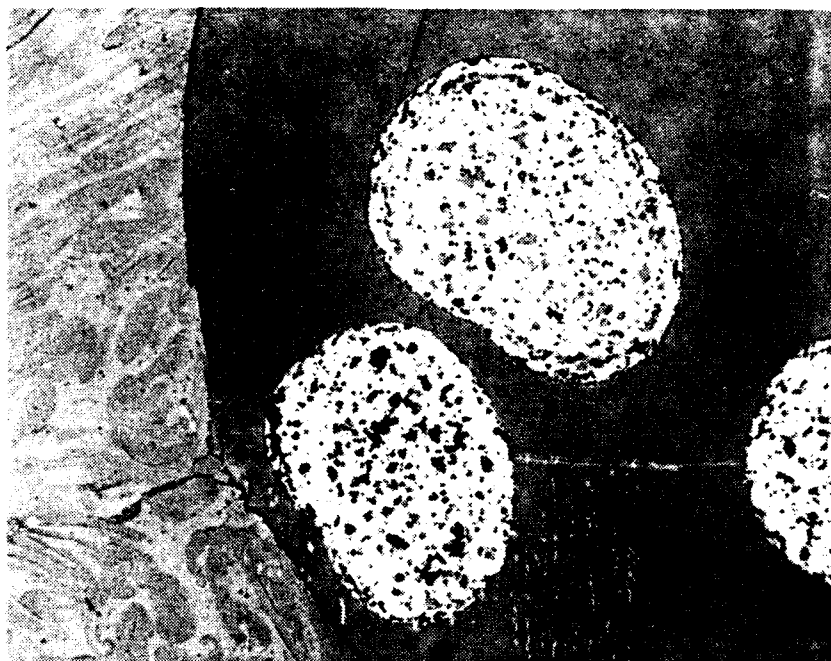
2-44

100μm
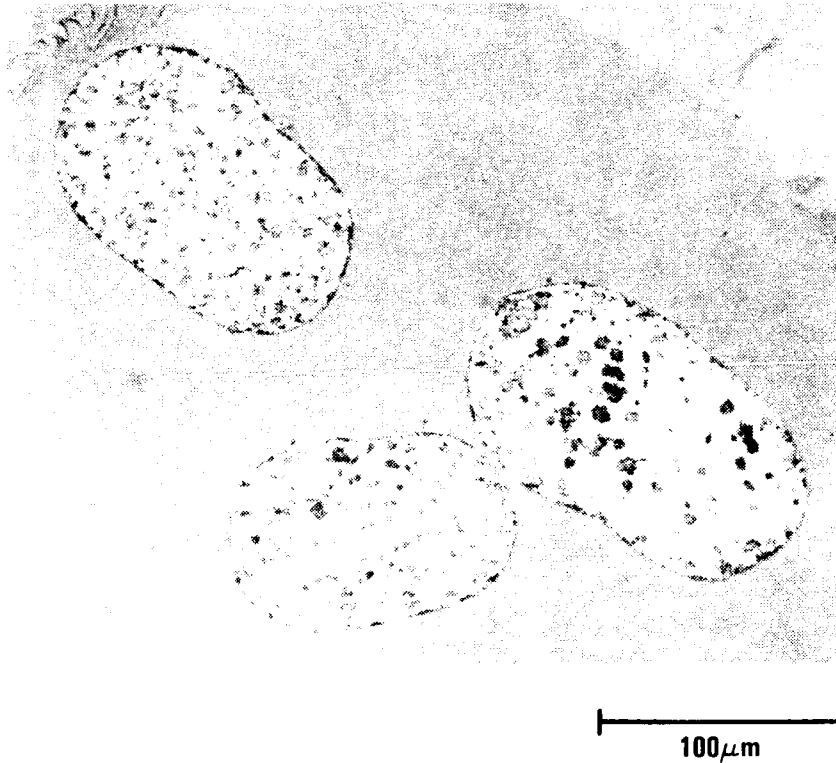
Fig. 25. The optical micrograph of the polished cross section of fiber
from batch 101056-85 II(Ag) calcined at the 900°C, 24 h
showing a large amount of porosity (Sample 10105-85 II (Ag)
H70,71,57; 300X; Jc = 201 A/cm^2)

30 wt % Y123 powder reduced the shrinkage from the original 50% to approximately 41%. The addition of Y123 powder, however, has an adverse effect namely it has a tendency to decrease draw-down ratio which results in a thicker fiber. Currently, the amount of Y123 powder addition to the resin is being optimized.

Preliminary results indicate that with the same heat treatment condition at 915°C for 24 h, the fiber has slightly bigger grain size as compared with fibers with no Y123 powder addition [Fig. 26(a) and (b)]. The fibers also exhibit current density up to 1920 A/cm^2.

Fig. 26. (a) Polished cross section of fiber with Y123 powder and silver addition with Jc = 1920 A/cm^2 using a nonpolarized light to show porosity and (b) polarized light to reveal grain size (400X)

3. ELECTROMAGNETIC PROPERTIES OF SOL-GEL DERIVED MATERIALS

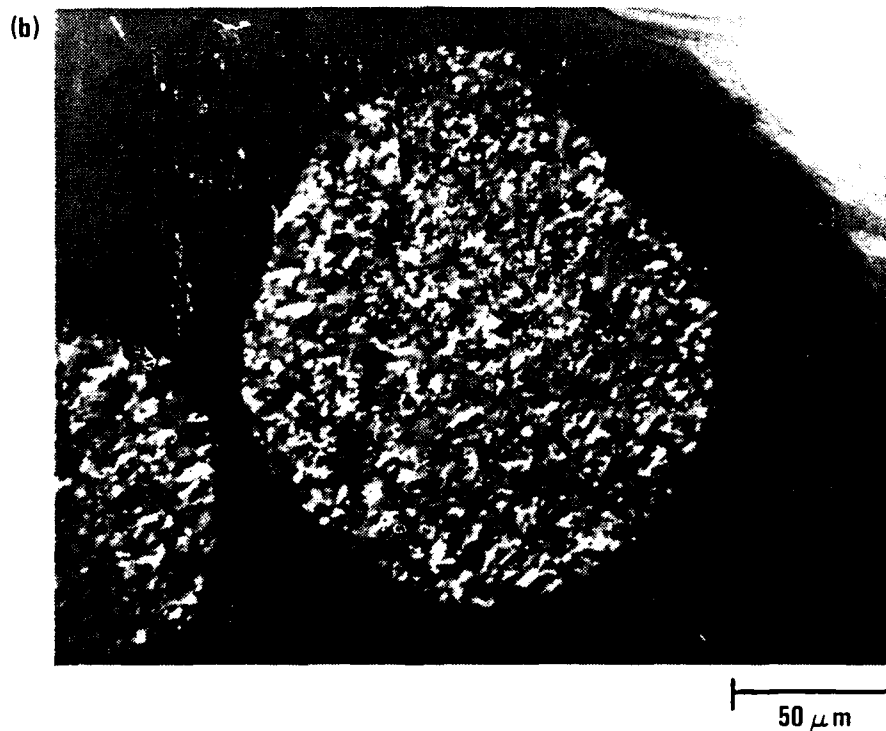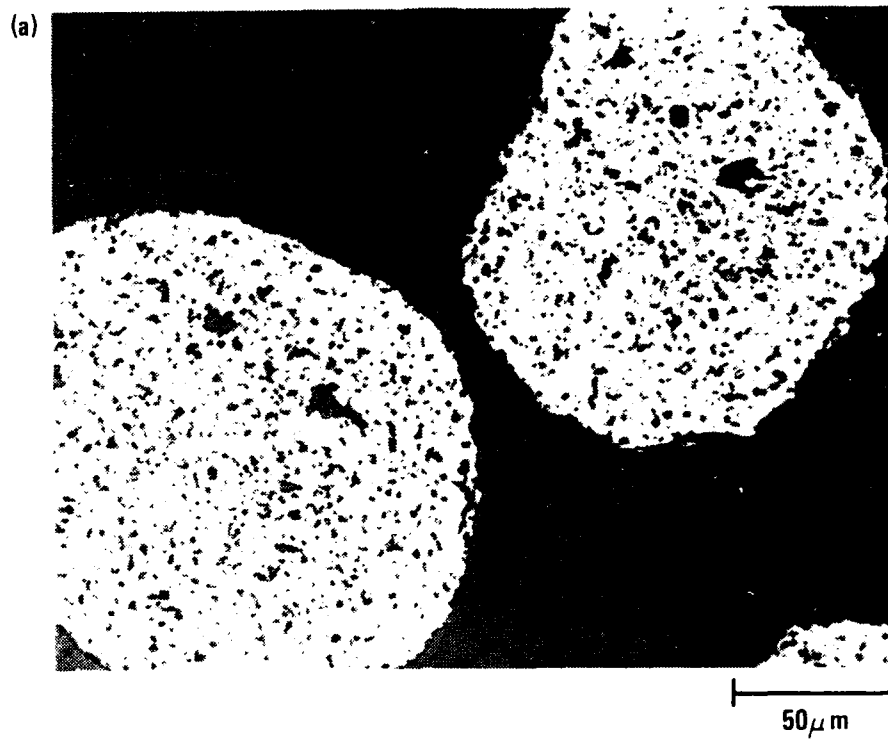A variety of electromagnetic property measurements, including dc magnetic susceptibility as a function of temperature, electrical resistivity as a function of temperature, and transport critical current density, have been made routinely performed on fibers and films prepared by sol-gel processes. In addition, a number of samples have been characterized by X-ray diffraction analysis, scanning electron microscopy, and electron microprobe analysis.

Electrical resistivity was measured at UCSD using a Linear Resistance LR-400 four-wire ac resistance bridge. Data were recorded with three Keithley 177 digital multimeters interfaced to an HP-85 computer. The current used for the measurements in this report was 1 μA.

Magnetic measurements were performed at General Atomics on a Quantum Design MPMS SQUID susceptometer.

Critical current was measured at UCSD in the absence of an applied field. Measurements were made using a four-wire dc technique with the sample immersed in liquid nitrogen. Equipment used included two Keithley 195A digital multimeters interfaced to a PC-AT compatible computer, a Kepco BOP 20-20M bipolar operational power supply and amplifier, and a Sorenson SRL 10-100 power supply. The critical current was determined using a criterion of 1 μV per cm as the voltage drop across the voltage leads.

Critical current was also measured as a function of temperature and applied field in a closed cycle refrigerator with He exchange gas at General Atomics using a four-wire ac technique. The cryostat,

model 257171A manufactured by APD Cryogenics, Inc., was equipped with an APD HC-2 compressor. The electromagnet, HV-7A, and power supply, HS-1356 4A, were manufactured by Walker Scientific. Equipment also included a Tektronic 5223 digitizing oscilloscope, a Tektronix FG 501A 2 MHz function generator, a Tektronix 016-0597-00 trigger generator, a Stanford Research SR560 low noise preamplifier, a Lakeshore DRC82C temperature controller, and a Kepco BOP 20-20M power supply. Again, the critical current criterion was a voltage drop of 1 μV per cm separation between voltage leads.

Other analytical equipment used at UCSD included a Rigaku Rotaflex RU-200B X-ray diffractometer, a Cambridge 360 scanning electron microscope, and a Cameca Instruments CAMEBAX electron microprobe. The standard used for determination of sample composition by electron microprobe was a polished polycrystalline sample whose superconducting properties were well established to be those of $YBa_2Cu_3O_{7-\delta}$ and whose composition had been compared to a single crystal of $YBa_2Cu_3O_{7-\delta}$.

3.1. FIBERS

Since the previous reporting period, fibers of $YBa_2Cu_3O_{7-\delta}$ have exhibited consistently high superconducting transition temperatures as measured by dc magnetic susceptibility and electrical resistivity. A summary of the electromagnetic measurements made on the $YBa_2Cu_3O_{7-\delta}$ fibers appears in Table 7. The maximum critical current density measured in liquid nitrogen in zero applied field was 2100 A/cm^2 (Fig. 27), and typical values were around 1000 A/cm^2. As shown in Fig. 28, the critical current density of a fiber doped with 3 wt % Ag was also measured as a function of temperature from 20 to 77 K in zero applied field and at H = 100 Oe. The Ag dopant allowed the fiber to be drawn finer, while maintaining a critical current density of 950 A/cm^2 at 77 K in zero applied field. At 21 K, J_c attained a value of 7500 A/cm^2 for H = 0, and a value of 880 A/cm^2 for H = 100 Oe. The fiber used in these

TABLE 7
YBa$_2$Cu$_3$O$_7$ FIBERS BY SOL-GEL METHOD
Summary of Electromagnetic Measurements

$T_c^{(a)}$

$T_{50,\rho} = 91.5$ K
$\Delta T_\rho = 1.5$ K

$T_{onset,\chi} = {>}90$ K
$T_{50,\chi} = 87$ K
$\Delta T_\chi = 10$ K
$\chi_{fc}/\chi_{zfc} = 0.31$

$J_c(0G, 77$ K$)^{(b)}$

typ. 10^3 A/cm^2
max. 2.1×10^3 A/cm^2

$J_c(H,T)^{(c)}$

See Figs. 27-28

---

[a] Reported first quarter 1990.

[b] Measurement performed in LN$_2$.

[c] Measurement performed in He vapor.
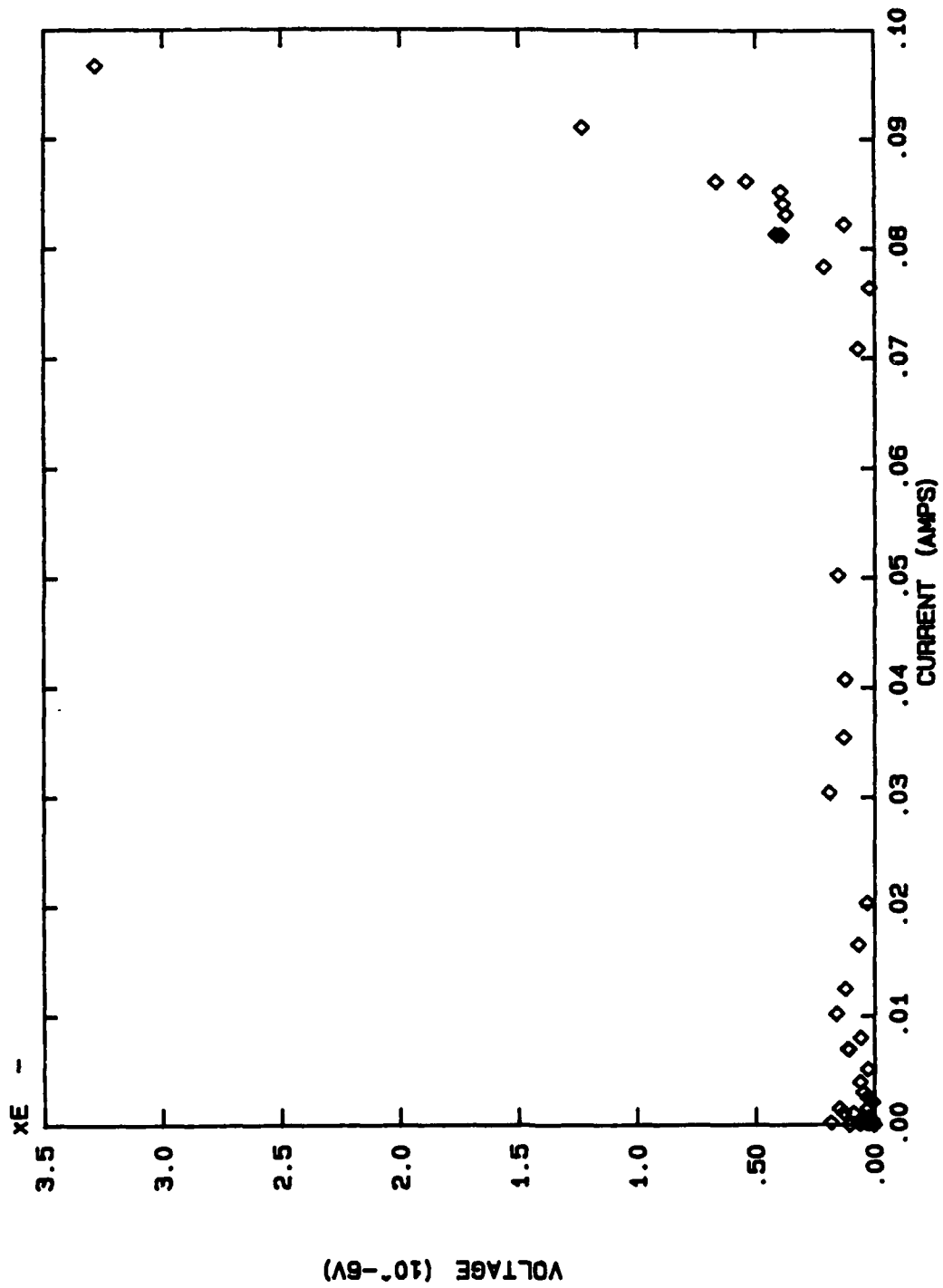
Fig. 27. Voltage as a function of current for an YBa$_2$Cu$_3$O$_7$-δ fiber at 77 K in the absence of an applied field. The critical current density was determined to be ~2100 A/cm^2 using a criterion of 1 μV/cm as the voltage drop across the voltage leads

Fig. 28. Critical current density as a function of temperature for an $YBa_2Cu_3O_{7-\delta}$ fiber at zero applied field and at H = 100 Oe. The fiber was doped with 3 wt % Ag. The critical current density was determined using a criterion of 1 $\mu V/cm$ as the voltage drop across the voltage leads

measurements had a diameter of 0.015 cm, and the separation between voltage leads was 0.183 cm.

3.2. THIN FILMS

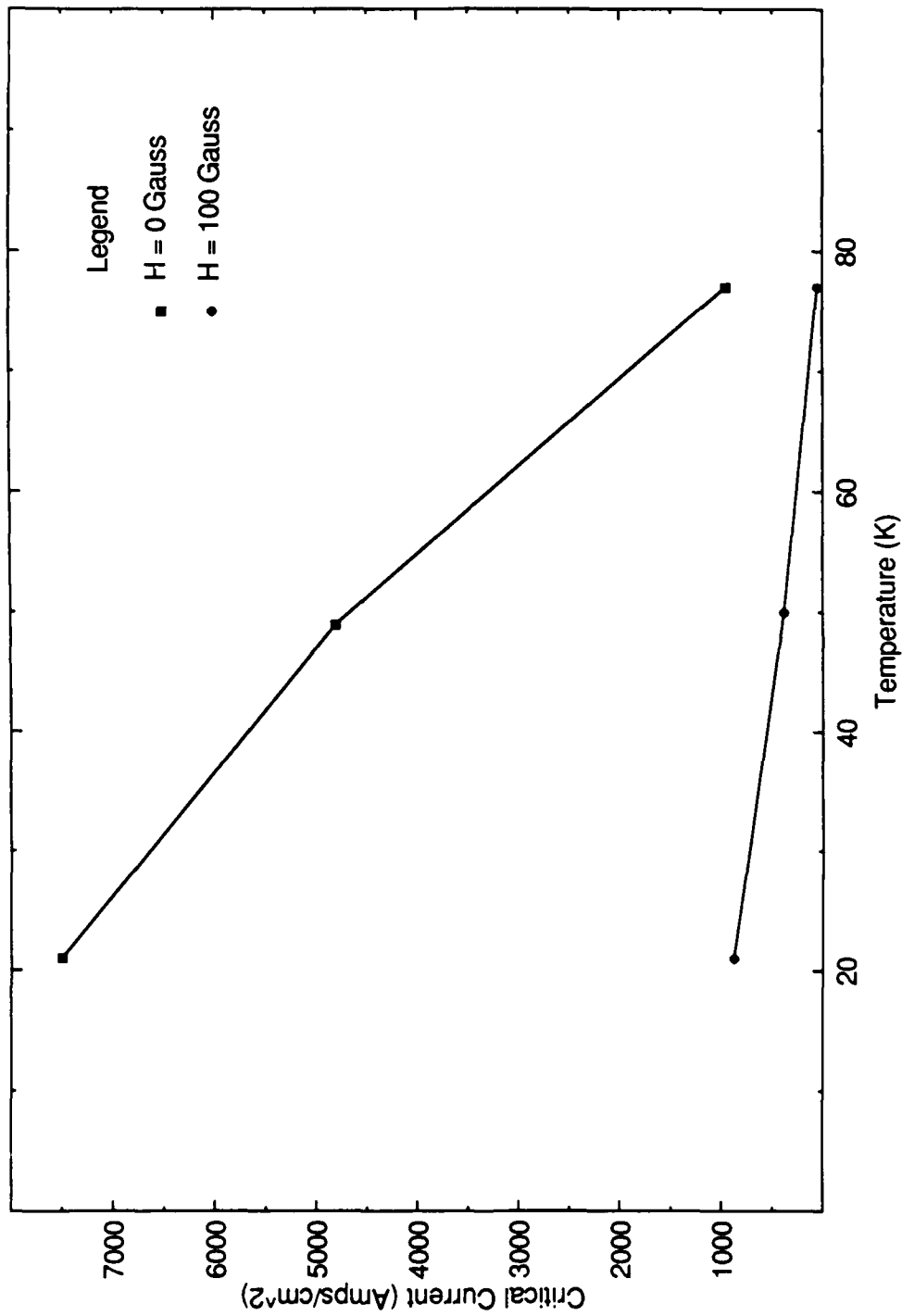Thin films of $YBa_2Cu_3O_{7-\delta}$ were made by two methods. In the first, the solvent is based on 2,2-ethoxy ethanol. The second method, which is potentially more cost-effective, uses a solvent based on toluene-isopropanol. Results are summarized in Table 8. Critical current densities are derived from order-of-magnitude estimates of the film thickness. Because zero resistance was achieved below liquid nitrogen temperature, J_c was measured at 30 K in zero applied field.

The first processing technique yielded more reproducible results. The best superconducting properties were obtained for films dipped on large-grained yttria-stabilized zirconia substrates and annealed in flowing O_2 at 921°C for 1 min and at 405°C for 24 h. As shown in Fig. 29, these films had high transition temperatures, $T_c = T_{50\%} = 91$ K and narrow transition widths $\Delta T = T_{90\%} - T_{10\%} = 4$ K as determined from electrical resistivity measurements. Transport critical current measured at 30 K in zero applied field was ~300 A/cm^2. X-ray diffraction showed some c-axis orientation. Electron microprobe analysis was performed on a number of thin films produced by this technique; considerable variations were found in the composition. Measurements of magnetic susceptibility were ambiguous, possible because the films were too thin or because of small grain size.

Two films with good superconducting properties were produced by the second processing method. X-ray diffraction measurements performed on these films showed a significant degree of c-axis orientation. Scanning electron microscopy on one of these films, dipped on a polycrystalline Ag substrate, revealed large (<10 μm) crystallites. Resistivity measurements of this film were not possible because of the high electrical conductivity of the Ag substrate. However, as shown in Fig. 30, dc

TABLE 8
$YBa_2Cu_3O_{7-\delta}$ THIN FILMS BY SOL-GEL METHOD

|	Method A 2,2-ethoxy ethanol sol	Method B Toluene-isopropanol sol	
Substrate	YSZ	Ag	$SrTiO_3(100$
Annealing	1 min @ 921°C 24 h @ 405°C	3 h @ 920°C 10 h @ 400°C	>1 min @ 825°C 19 h @ 400°C
T_c	$T_{50,\rho} = 91$ K $\Delta T_\rho = 4$ K	$T_{50,\chi} = 63$ K $\Delta T_\chi = 52$ K $T_{onset} = 85\text{-}90$ K $\chi_{fc}/\chi_{zfc} = 0.50$	$T_{50,\rho} = 77$ K $\Delta T_\rho = 12$ K
Structure	$I_{006}/I_{012} \leq 3$	$I_{006}/I_{012} = 200$ Flat crystallites ≤ 10 μm	$I_{006}/I_{012} = 23$ Fine grains ~1 μm
Y:Ba:Cu	Variations in composition; some spots close to 1:2:3		1:2.3:6.3
J_c (0 G, 30 K)	300 A/cm^2		400 A/cm^2
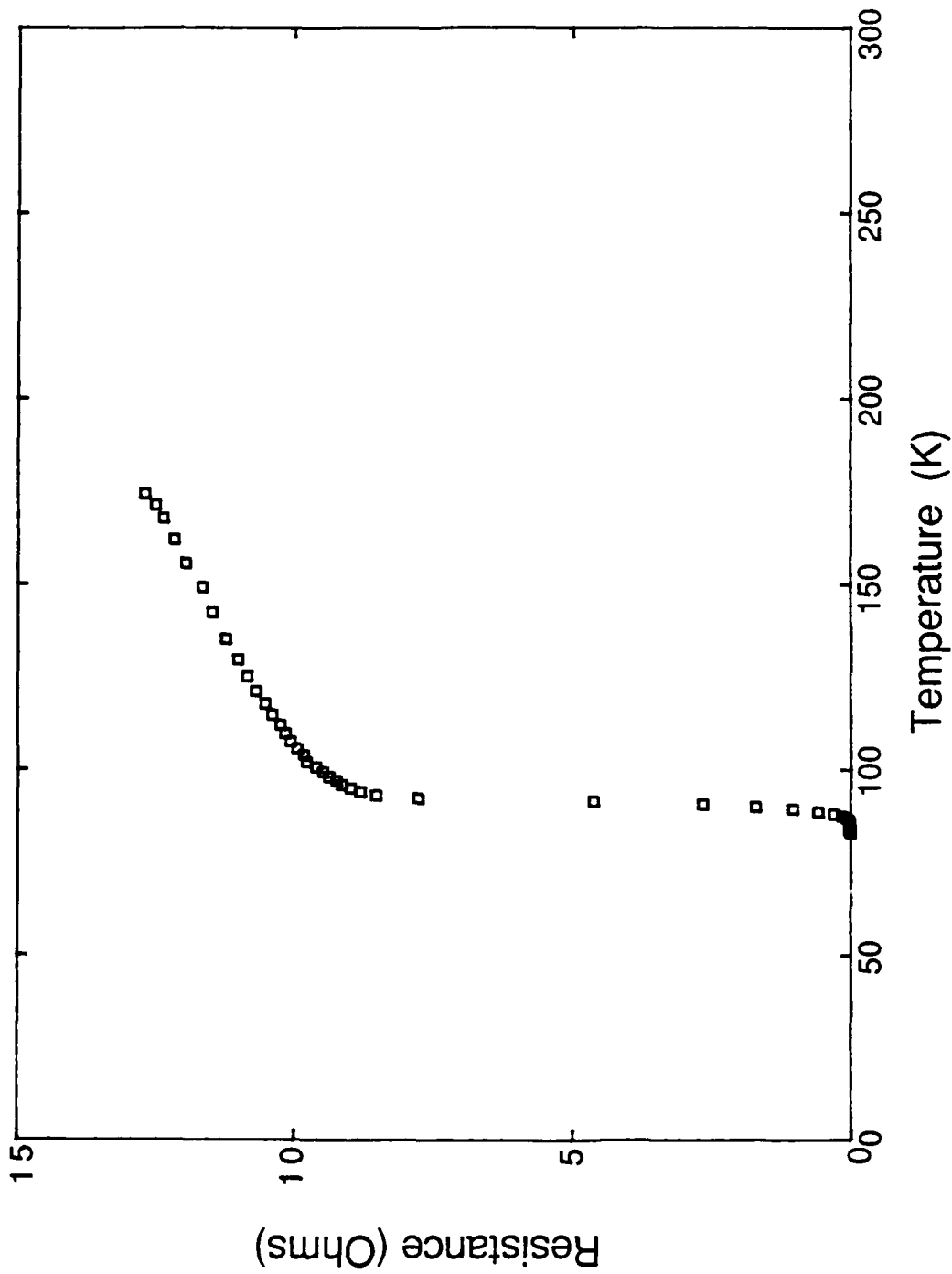
Fig. 29. Resistivity as a function of decreasing temperature for an $YBa_2Cu_3O_{7-\delta}$ thin film on large-grained yttria-stabilized zirconia. The superconducting transition occurred with a midpoint at 91 K and a width of 4 K
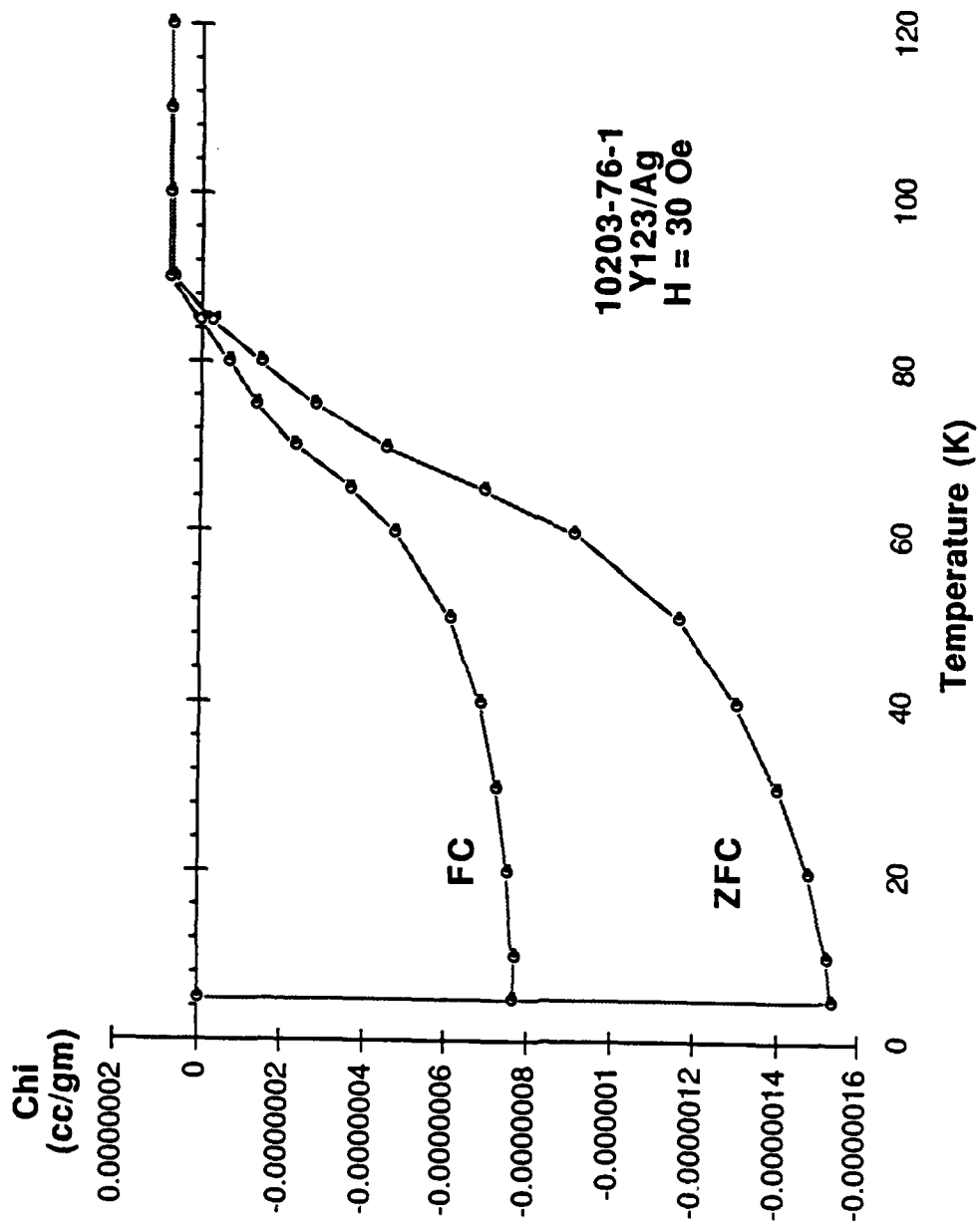
Fig. 30. Magnetic susceptibility as a function of temperature for an YBa$_2$Cu$_3$O$_{7-\delta}$ thin film on polycrystalline Ag. The sample was cooled in zero field to 5 K, a field of 30 Oe was applied, and the sample was heated to 120 K and cooled to 5 K. The superconducting transition occurred with an onset above 85 K, a midpoint at 63 K, and a width of 52 K.

magnetic susceptibility revealed the onset of superconductivity between 85 and 90 K. The other film, $YBa_2Cu_3O_{7-\delta}$ dipped on a $SrTiO_3(100)$ substrate, was smooth with uniformly small grain size. Microprobe analysis on this film showed an excess of copper. Since the copper was not detectable by X-ray diffraction, we conclude that it may have existed in nano crystalline form in the intergranular region. While the reproducibility of this technique has not yet been demonstrated, the results are promising.

4. CAVITY Q FACTOR MEASUREMENT

A longer copper cavity, consisting of two end plates and an open cylinder just like a metal cavity coated on the inside with high temperature superconducting ceramic (HTSC) was constructed. The new cavity is 1.35 in. long and its resonant frequency is 10.1 GHz. The new cylinder was electropolished. The temperature dependence of the Q of this new cavity was obtained. The Q was 40,000 at 77 K and 62,000 at 29 K.

The temperature dependence of the surface resistance of a HTSC coating on a 0.5 in. diameter silver disk relative to an uncoated, polished silver disk of the same size was measured. As shown in the Fig. 31, though the Q of the cavity with the coated disk improved dramatically as the temperature was decreased below 85 K, the coating was found to have a substantially higher surface resistance than silver.

The kit for screening up to four superconducting films by obtaining the temperature dependence of the ac magnetic susceptibility has arrived from Lakeshore Cryogenics. An insert for our liquid helium dewar has been designed and is now being built. As shown in the detailed drawings in the appendix, this insert will be used for both ac susceptibility and microwave surface resistance measurements. The software provided with the screening kit must be converted (from GW Basic with National Instruments subroutines to HP Basic) to run on our personal computer; this is mostly a matter of changing all the input and output commands and it will be started in June.
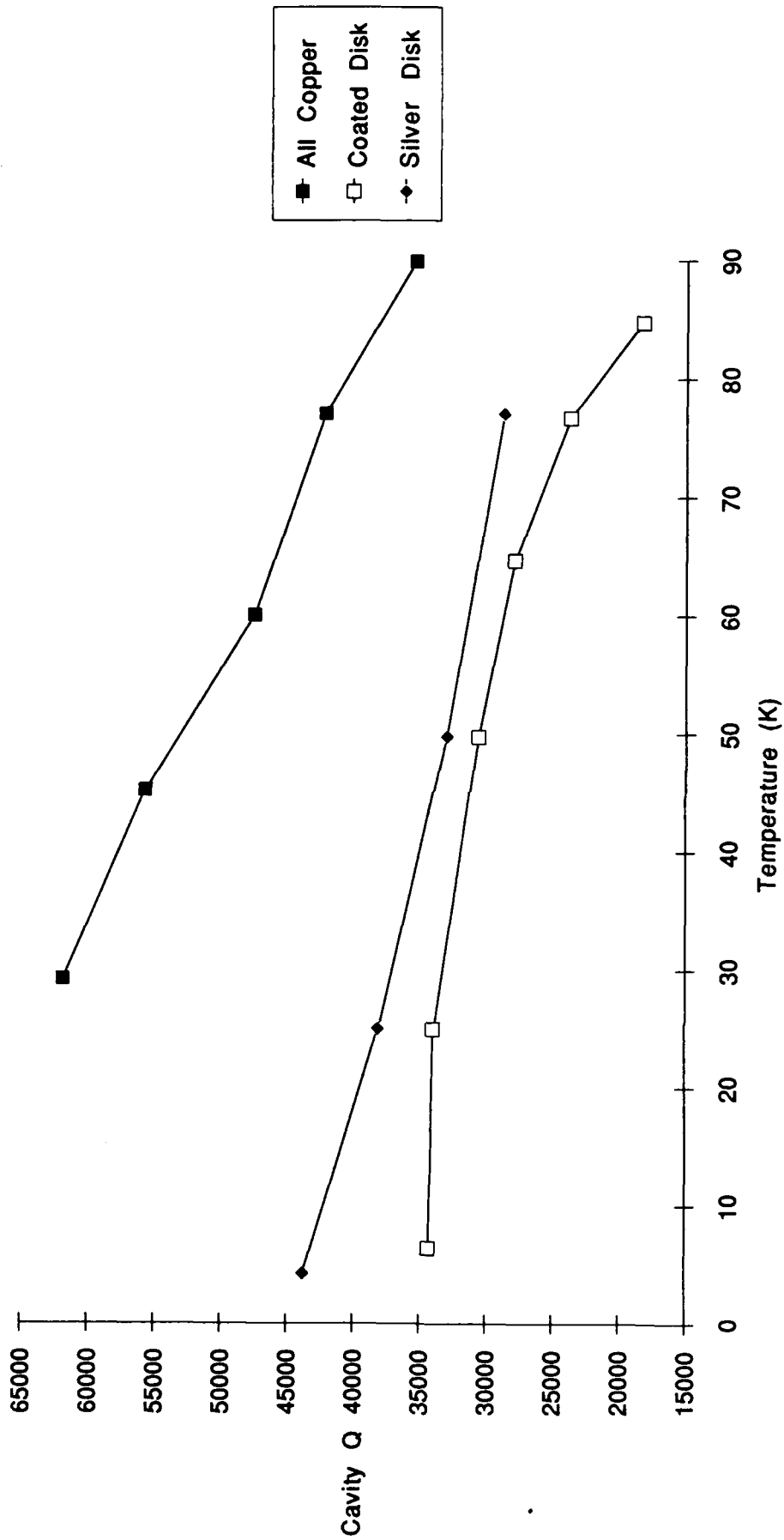
Fig. 31.

4-2

5. REFERENCES

1. Fahrenholtz, W. G., D. M. Millar, and D. A. Payne, "Preparation of $YBa_2Cu_3O_{(7-x)}$ from Homogeneous Metal Alkoxide Solution," Advanced Ceramic Materials, preprint.

2. Mazdiyasni, K. S., et al., "High Temperature Ceramic Superconductors for Period January 1, 1990 - March 31, 1990," General Atomics report GA-C19465, April 10, 1990.

3. Naito, M., et al., J. Material Research, 2(6), 713 (1987).

4. Cheung, C. T., and E. Ruckenstein, "Superconductor-Substrate Interactions of the Y-Ba-Cu Oxide," J. Materials Research, 4(1), 1 (1989.)

5. Mazdiyasni, K. S., "Powder Synthesis from Metal-Organic Precursors," Ceramic International, 8(2), 42-56 (1982).

APPENDIX A
NEW DESIGN OF CRYOSTAT FOR CHARACTERIZING HTSC MATERIALS
FOR DARPA/ONR CERAMIC SUPERCONDUCTOR PROGRAM

5 liter Superinsulated Liquid Helium Dewar with Insert

Boil-off to be ≤ 1.8 liters/day

LIQUID HELIUM 5.5 LITERS

3.25 DIA

4.25 DIA

48.0
44.0
24.0
20.0
6.00
7.50
4.00
4.00
4.00
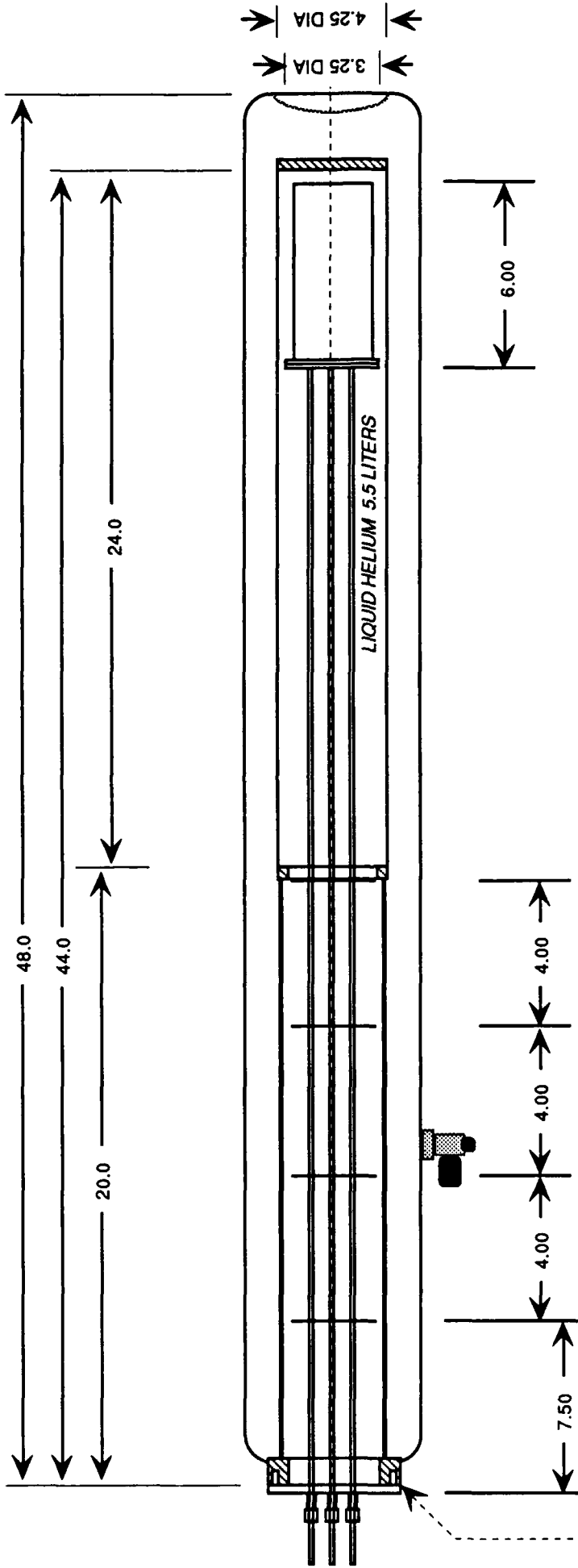
O-RING #2-240
I.D. = 3.750
W.D. = 0.180
DP. = 0.104

#8-32 TAP x 0.500 DP.
6-PLCS. EQ SPA. ON A
4.625 DIA B.C. (HELICOIL)

A-2

ALL DIMENSIONS ARE IN INCHES

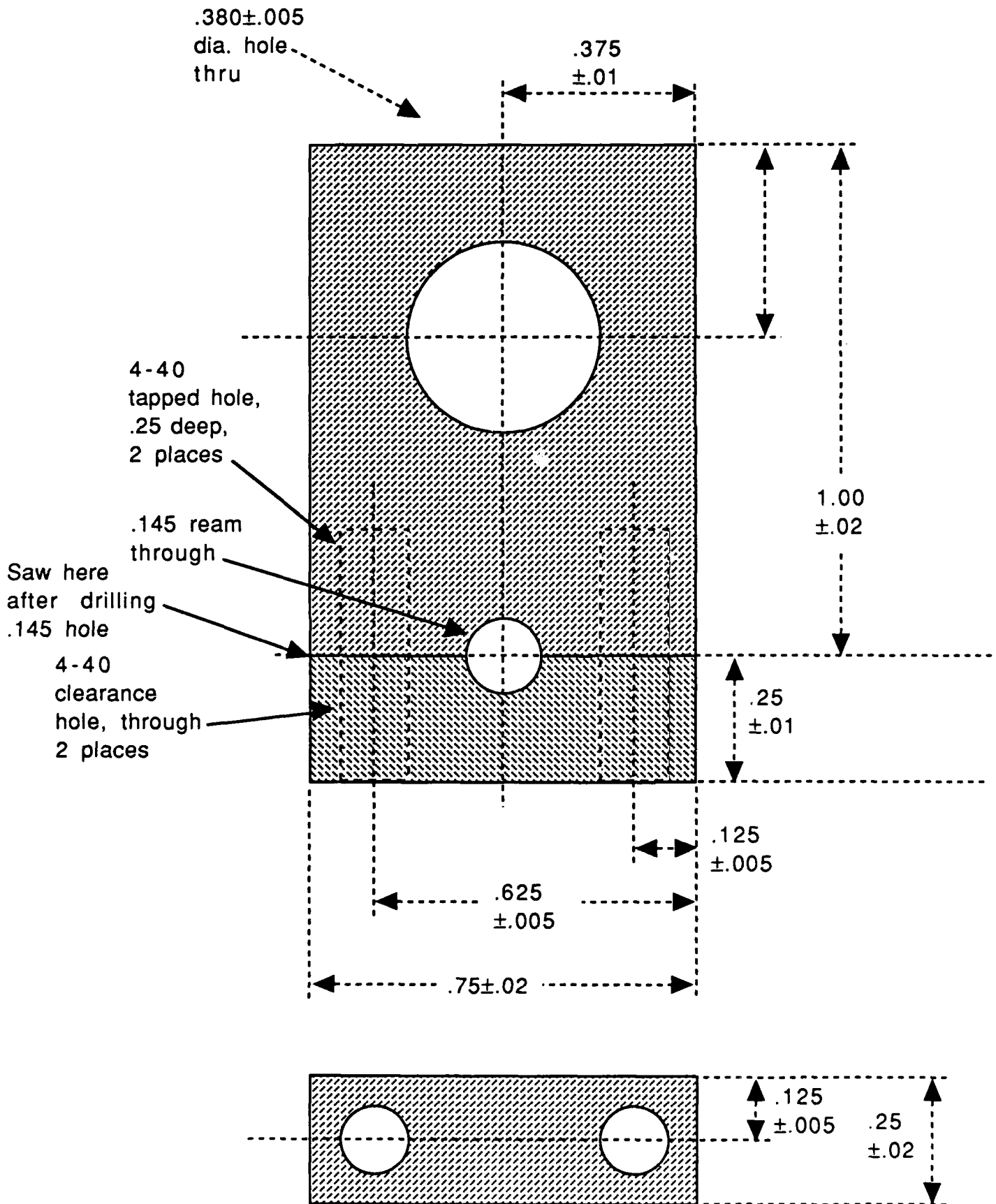Insert for 5 Liter Dewar

6.00

17.5

21.5

25.5

29.5

44.0

ALL DIMENSIONS ARE IN INCHES

A-3

Clamp for Coaxial Cable

Mat'l: aluminum
This clamps to coaxial cable. Micrometer is mounted in .375 hole.

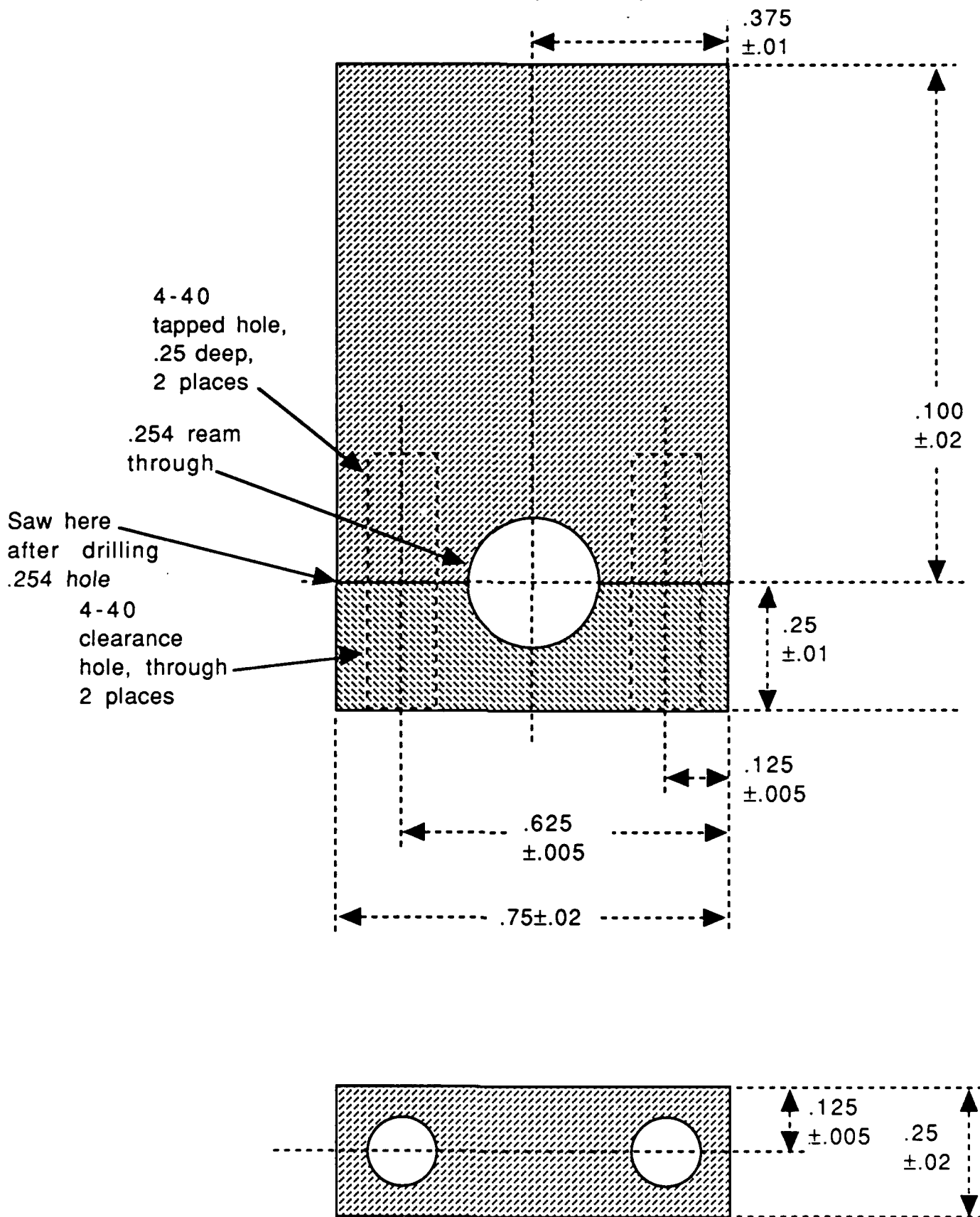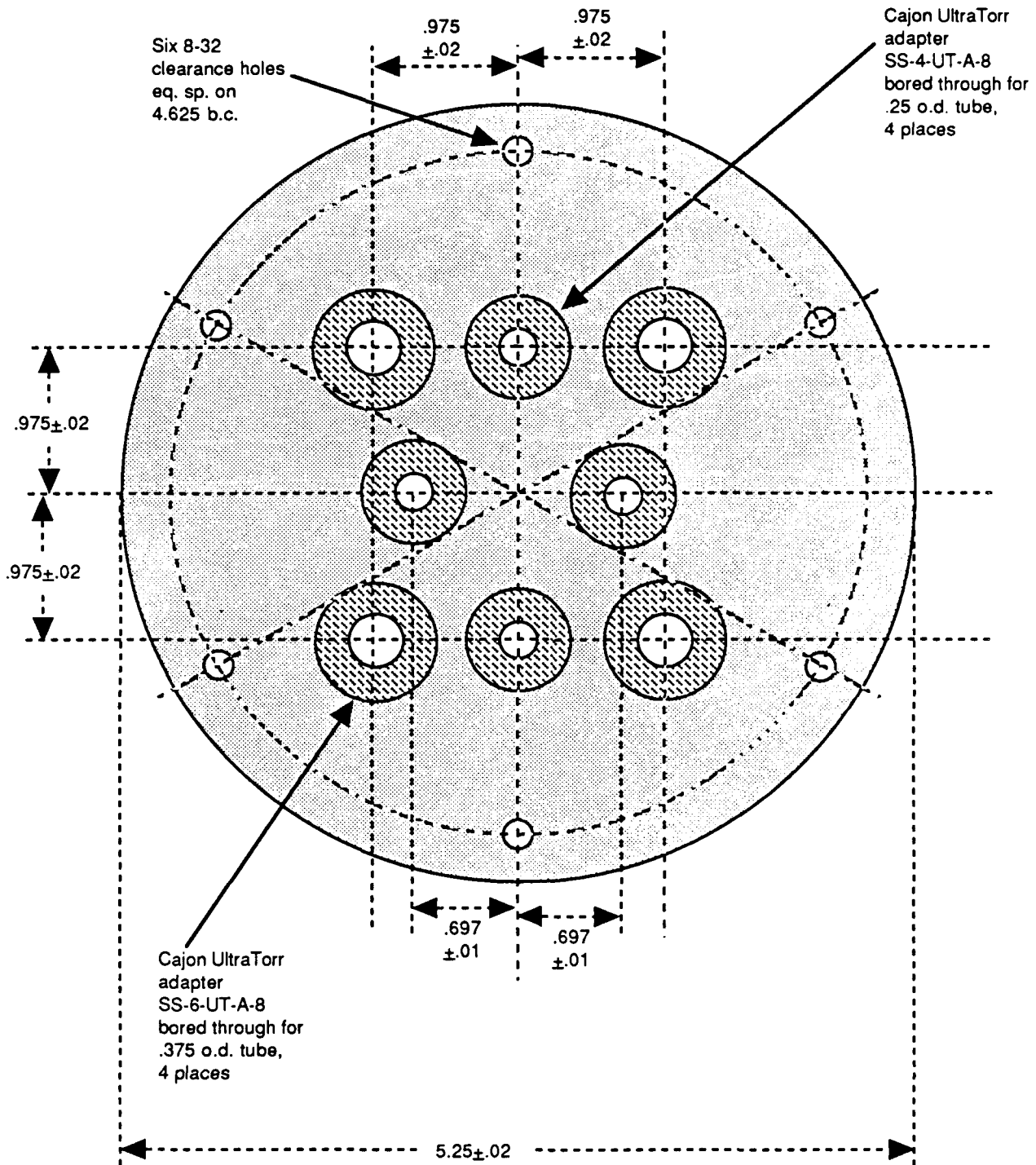.380±.005
dia. hole
thru

.375
±.01

4-40
tapped hole,
.25 deep,
2 places

.145 ream
through

Saw here
after drilling
.145 hole

4-40
clearance
hole, through
2 places

1.00
±.02

.25
±.01

.125
±.005

.625
±.005

.75±.02

.125
±.005

.25
±.02

A-4

Clamp for Tube

Mat'l: aluminum

This clamps to .025 o.d. tube. Micrometer pushes against it.

.375
±.01

4-40
tapped hole,
.25 deep,
2 places

.254 ream
through

Saw here
after drilling
.254 hole

4-40
clearance
hole, through
2 places

.100
±.02

.25
±.01

.125
±.005

.625
±.005

.75±.02

.125
±.005

.25
±.02

Vacuum Assembly Top (Height Adjustable)

Six 8-32
clearance holes
eq. sp. on
4.625 b.c.

.975
±.02

.975
±.02

Cajon UltraTorr
adapter
SS-4-UT-A-8
bored through for
.25 o.d. tube,
4 places

.975±.02

.975±.02

.697
±.01

.697
±.01

Cajon UltraTorr
adapter
SS-6-UT-A-8
bored through for
.375 o.d. tube,
4 places

5.25±.02

Mat'l: .250 thick stainless steel.

This is bolted onto the top of the dewar.

Baffle

.25 dia. hole
through on
.975 radius
at approx.
45 degrees

.26 dia hole
thru (for
soldering to
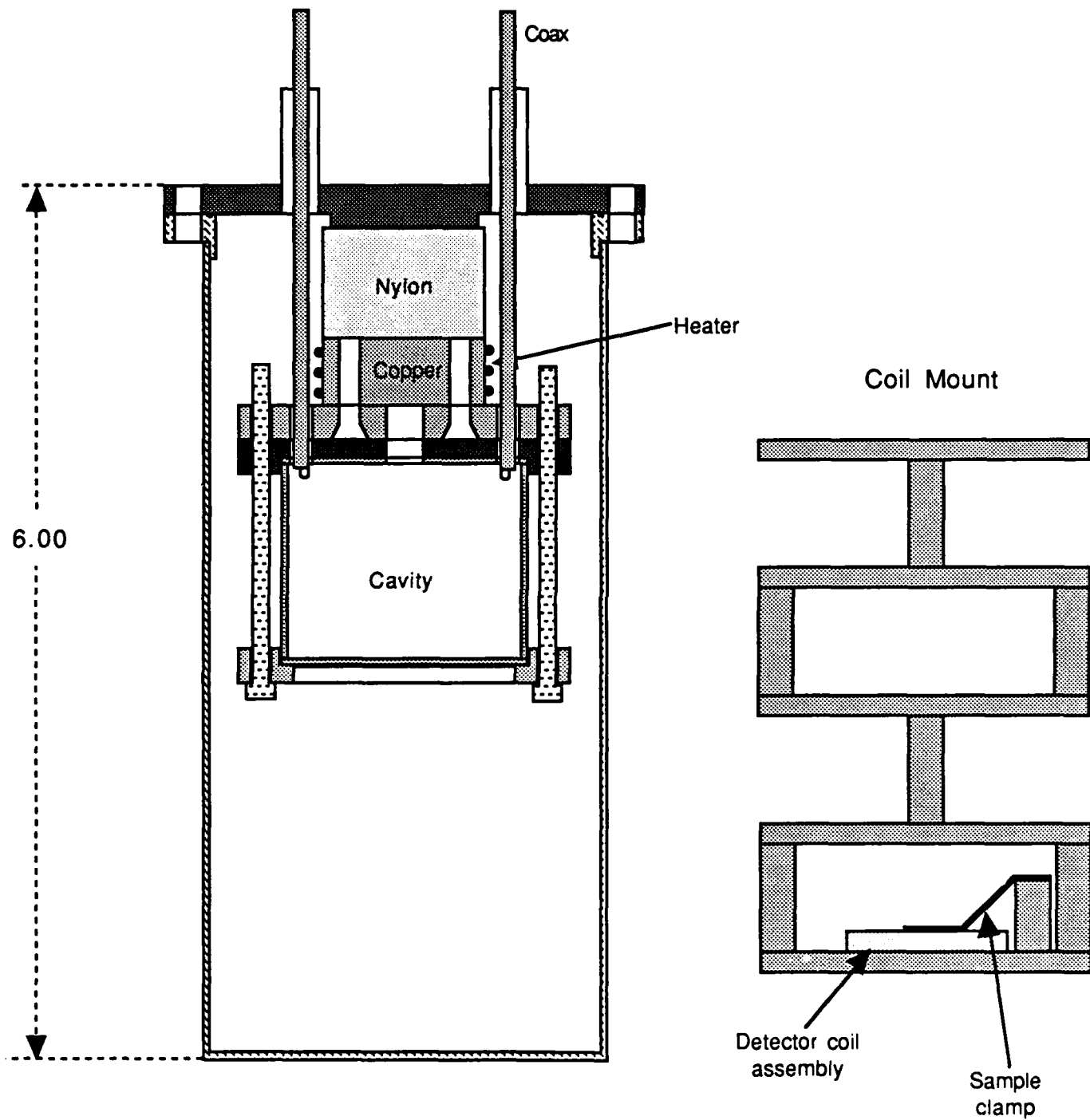.25 o.d. tube),
4 places

.975
±.02

.975
±.02

.697
±.01

.697
±.01
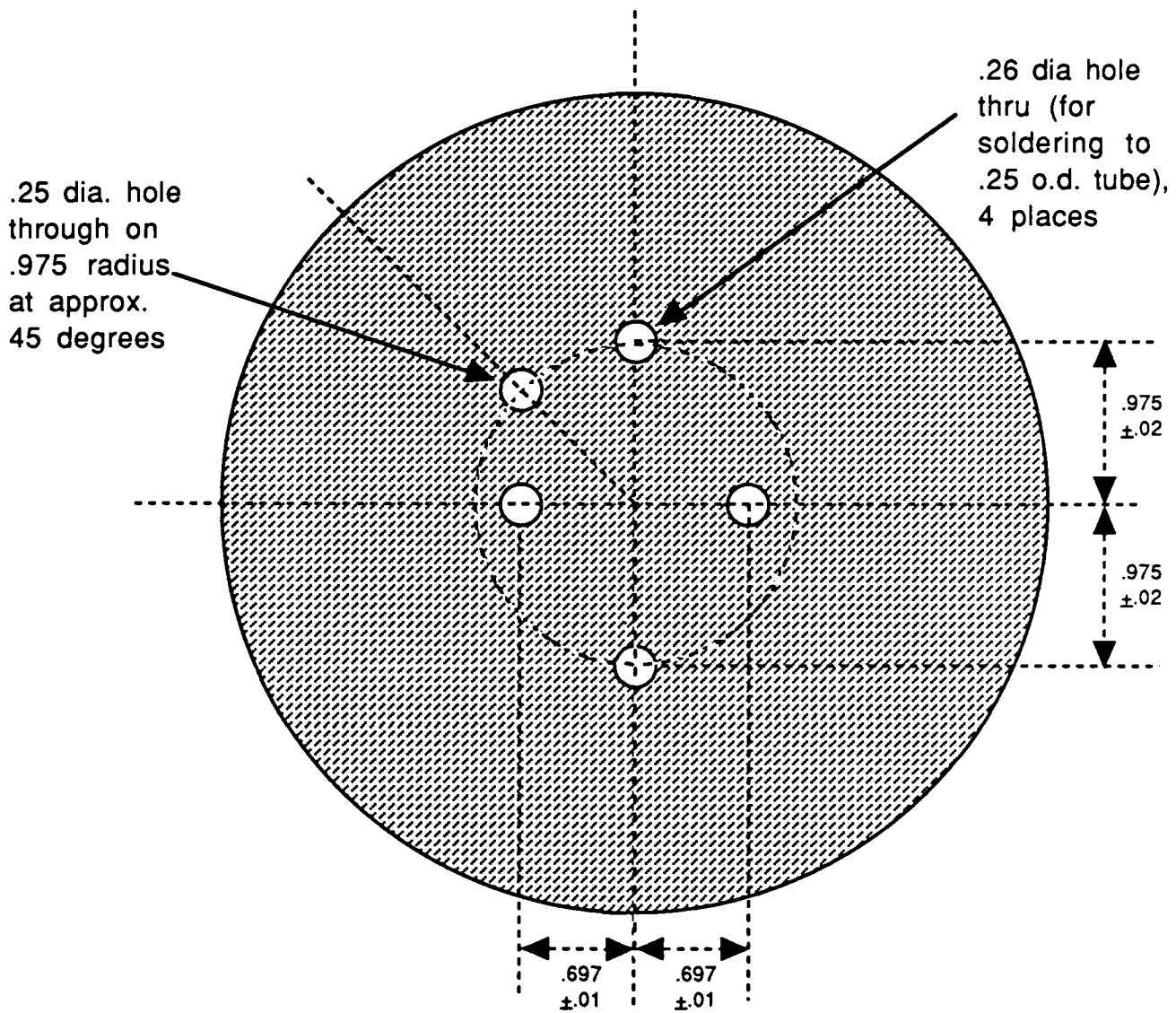
Mat" .050 thick brass.

Four of these are soldered to the .25 o.d. stainless
tubing where indicated in insert assembly drawing.

Vacuum Can Assembly
With Cavity or Coils

Coax

Nylon

Copper

Heater

6.00

Cavity

Coil Mount

Detector coil
assembly

Sample
clamp

Vacuum Can Lid
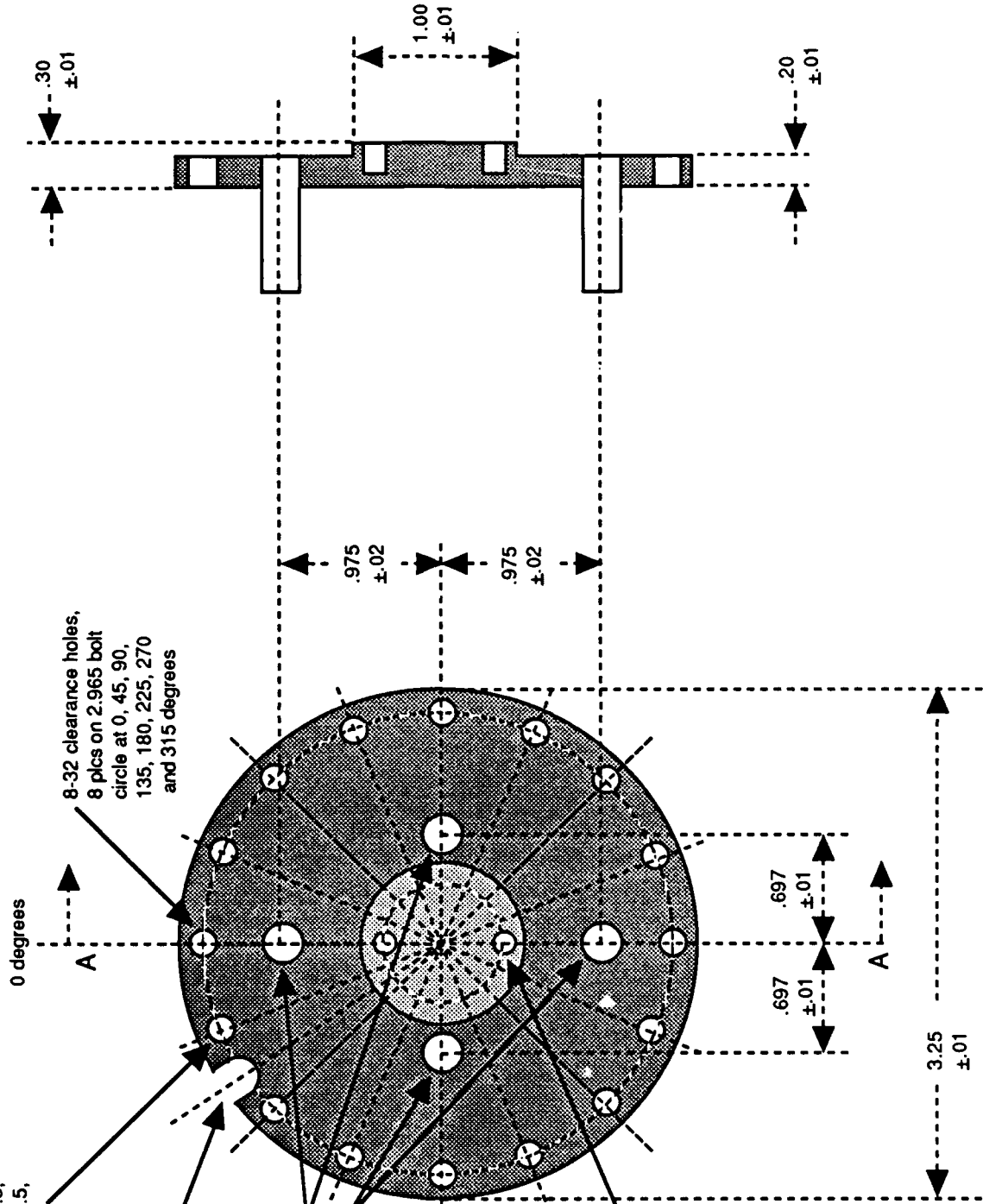
Mat'l: stainless steel

.30 ±.01

1.00 ±.01

.20 ±.01

.975 ±.02

.975 ±.02

8-32 tapped holes,
8 plcs on 2.965 b.c.
approximately
at 22.5, 67.5, 112.5,
157.5, 202.5, 247.5,
292.5, and 337.5

8-32 clearance holes,
8 plcs on 2.965 bolt
circle at 0, 45, 90,
135, 180, 225, 270
and 315 degrees

0 degrees

A

.697 ±.01

.697 ±.01

3.25 ±.01

A

0.30±.01 deep cut out
with .26 radius at
about 38 degrees

.25 O.D.
thin wall
stainless
steel tubing
welded in
four places

Two 6-32 tapped
holes, .20 deep,
on 0.750 bolt
circle at 0 and
180 degrees

A-9

Vacuum Can Assembly

.300
±.005

2.750 O.D.

2.650 I.D.

5.80

Vacuum Can Flange

8-32 tapped holes,
.250 deep,
equally spaced 8 plcs
on 2.965 bolt circle

.040 wide, .020 deep
groove for Indium O-ring

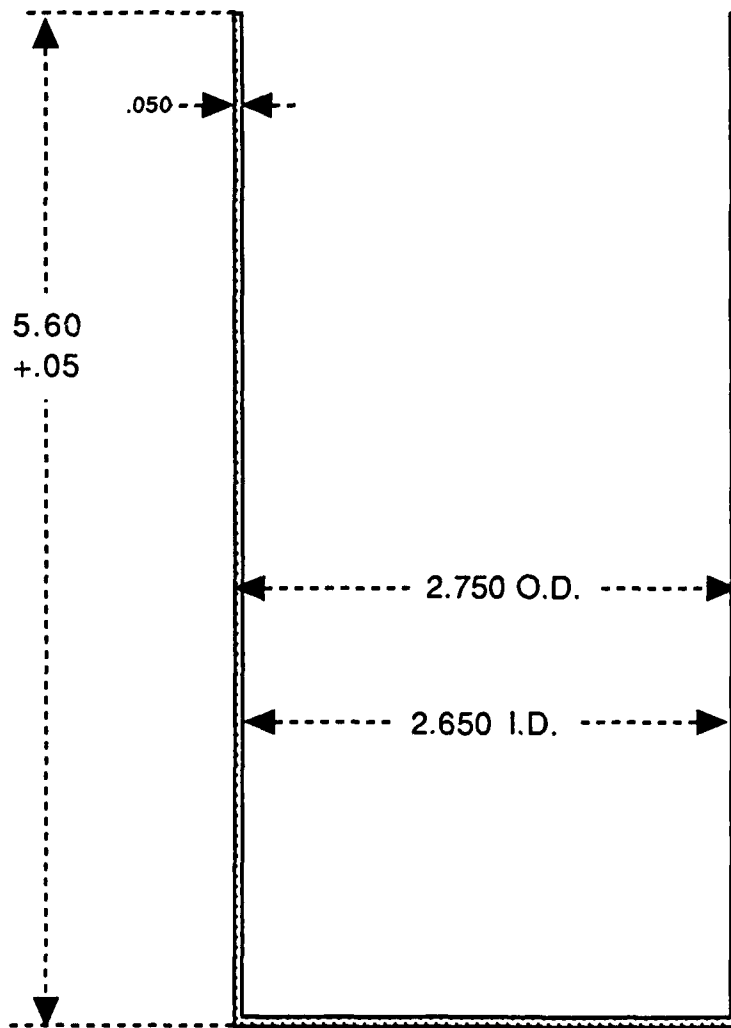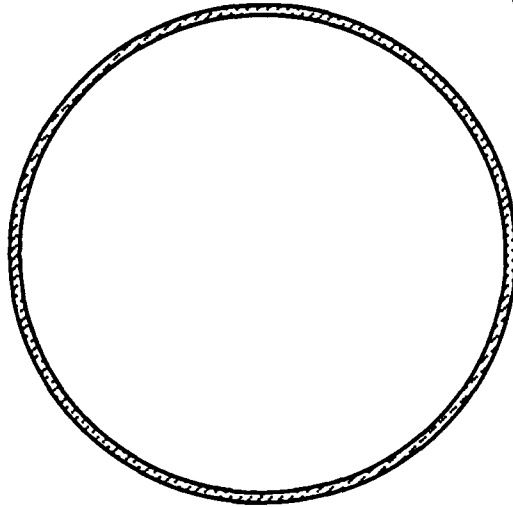2.540

2.640

2.680

3.250

.300
±.005

.325
±.005

.125
±.005
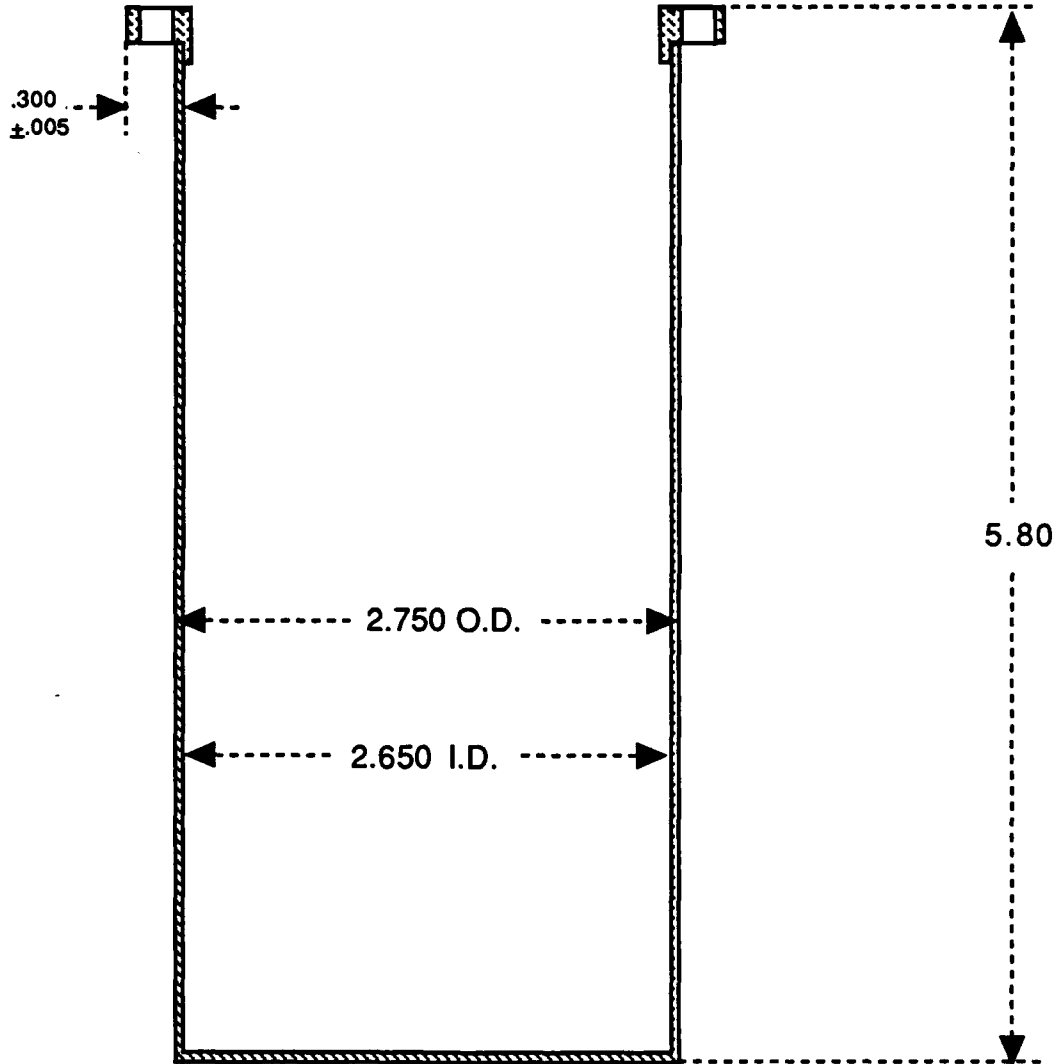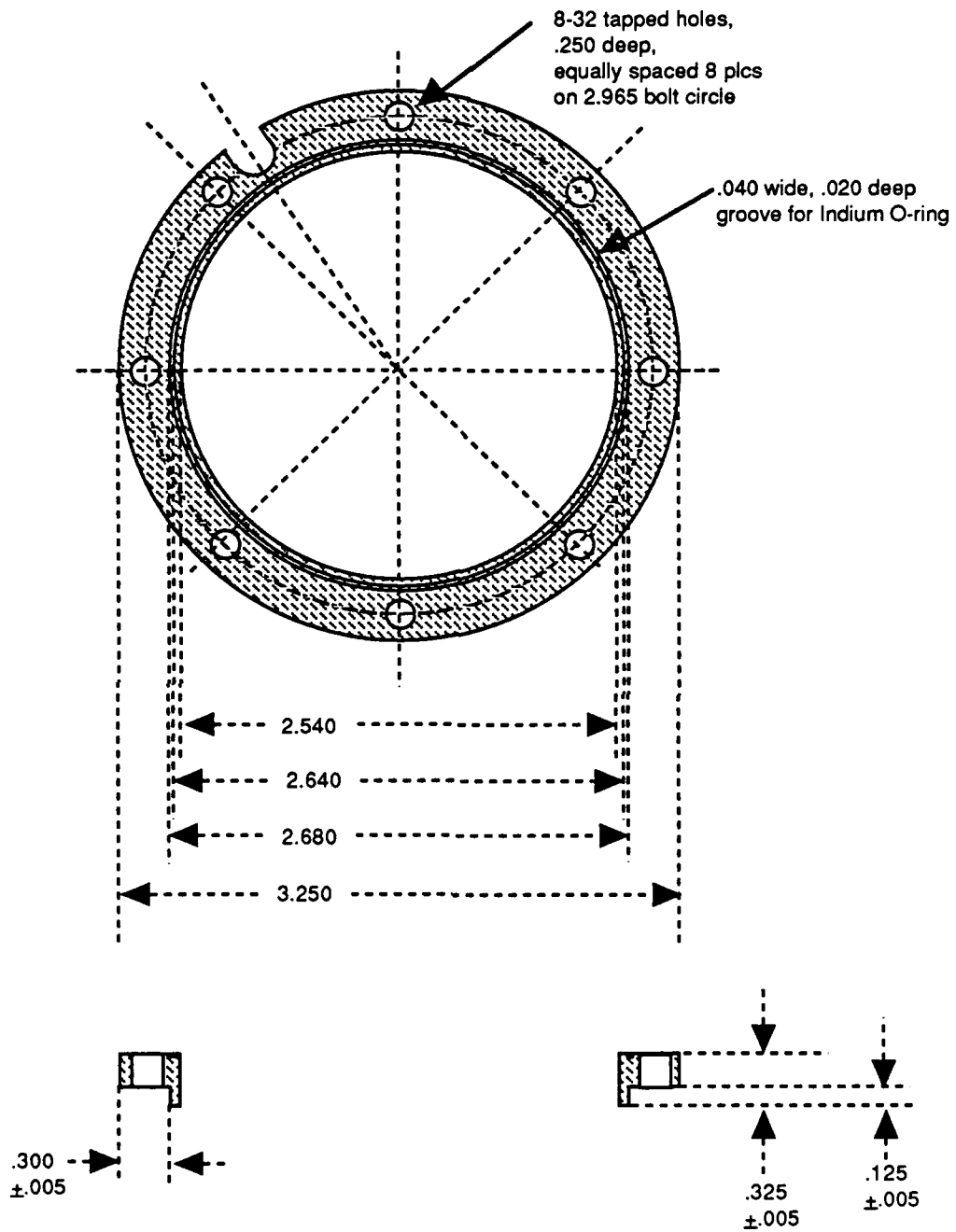
Mat'l: stainless steel.

Vacuum can lid is bolted onto this. This is welded to
vacuum can to make vacuum can assembly.

Mat'l:
stainless steel.

Vacuum Can

Welded to
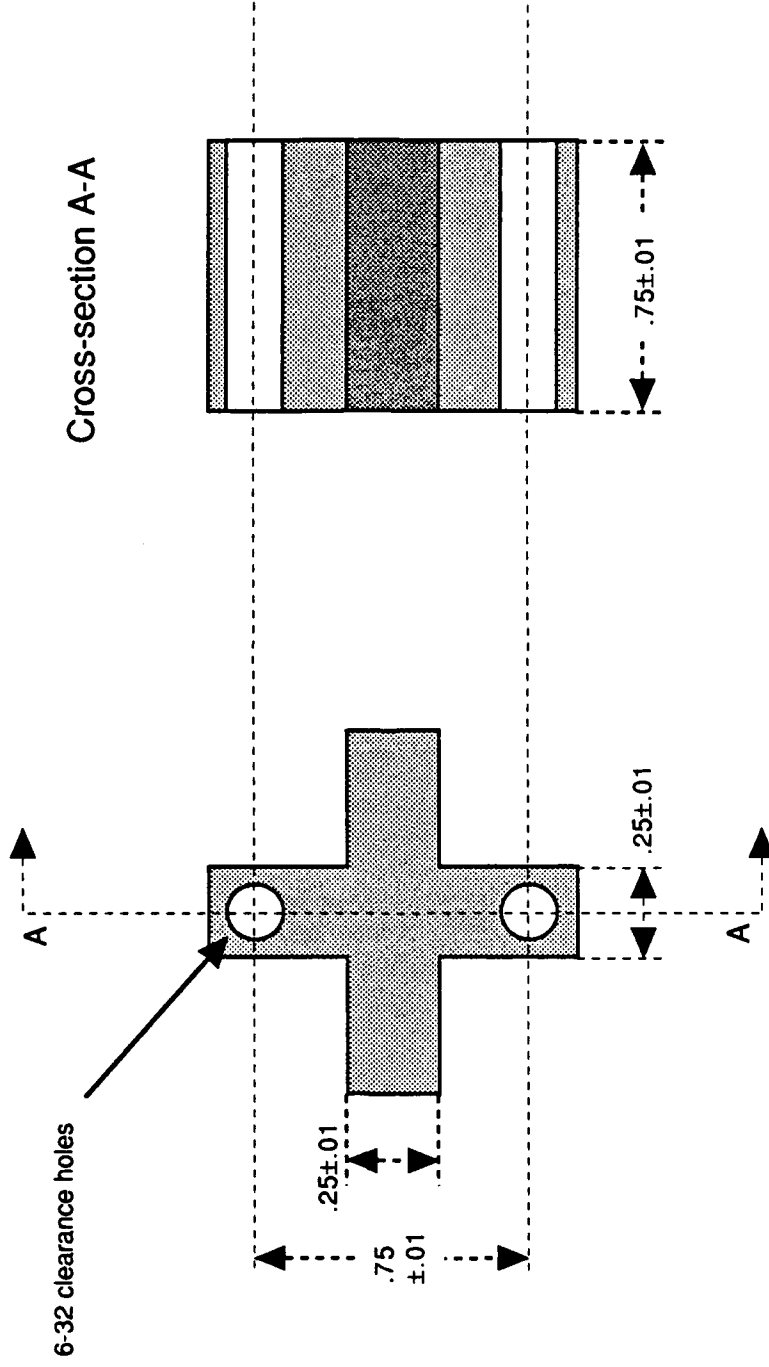vacuum can
flange to
make vacuum
can assembly.

.050

5.60
+.05

2.750 O.D.

2.650 I.D.

Thermal Standoff

Mat'l: Nylon

Heat sink is bolted onto this. This is bolted onto vacuum can lid.

6-32 clearance holes

.25±.01

.75 ±.01

Cross-section A-A

.75±.01

.25±.01

A

A

Heat Sink

Mat'l: copper

Mounting plate is bolted onto this. This is bolted onto thermal standoff. Heater is wrapped around this.

0 degrees
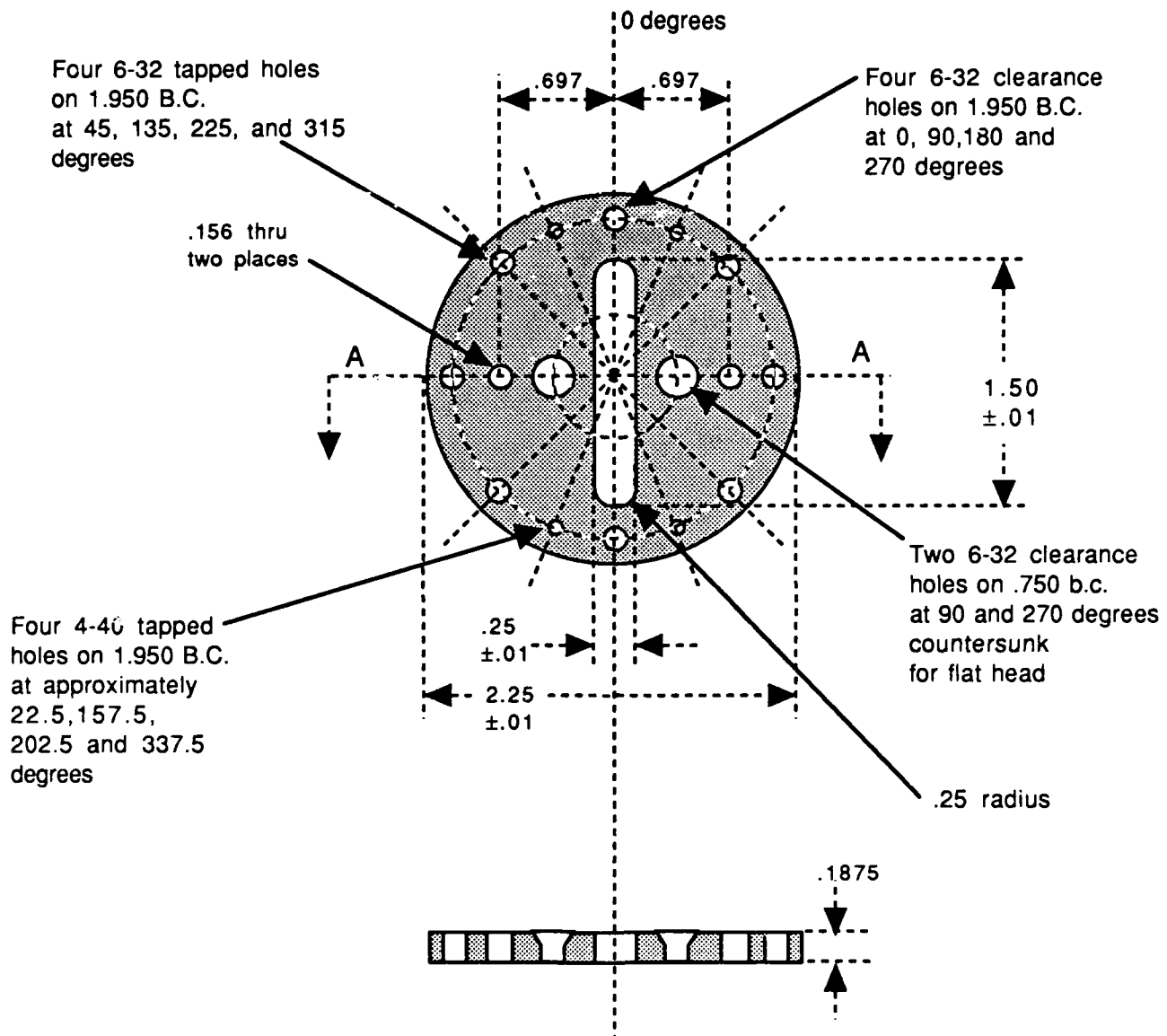
6-32 clearance holes, countersunk for flat head, at 0 and 180 degrees on .750 b.c.

A

A

6-32 tapped holes at 90 and 270 degrees on 0.750 b.c.

1.10±.01

.45 ±.01

Cross-section A-A

A-14
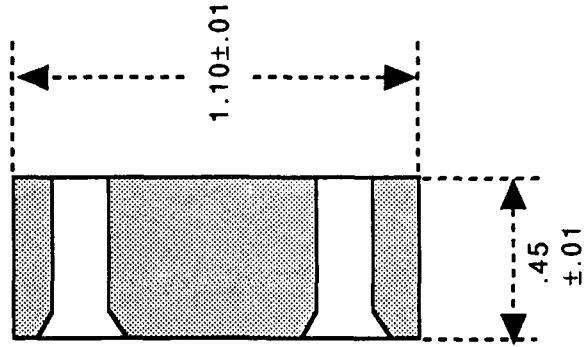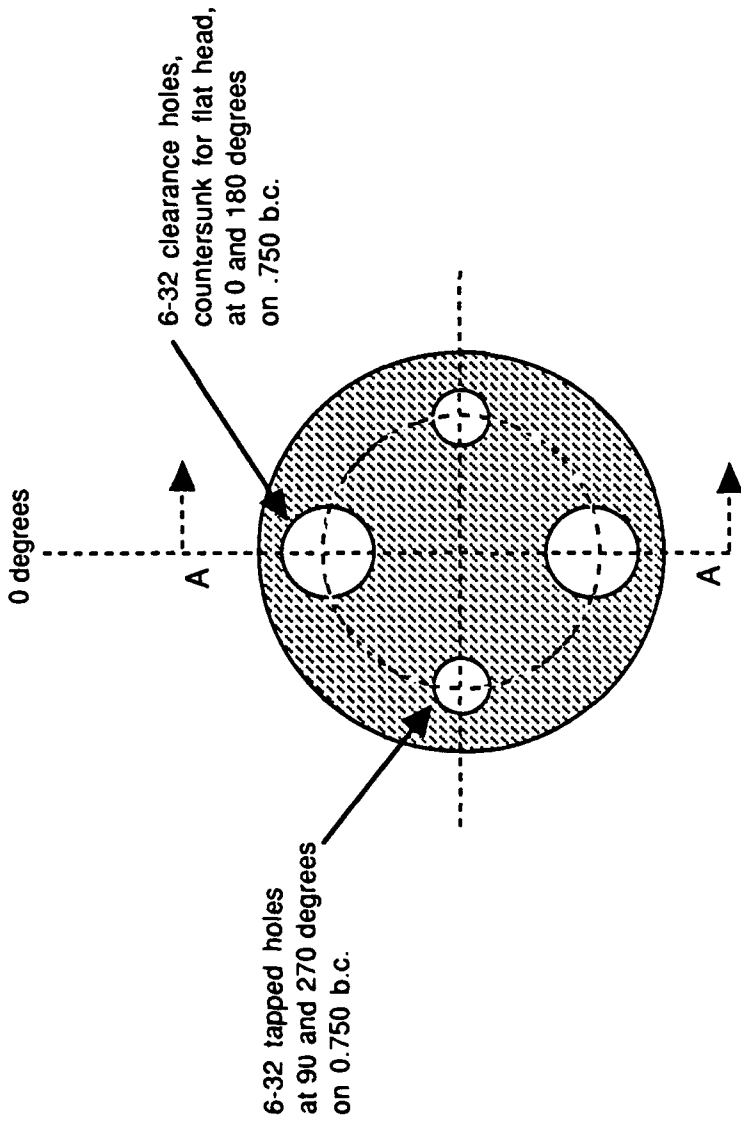
Mounting Plate

Mat'l: copper
This is bolted onto heat sink. Cavity frame or sample mount bolts onto this.

0 degrees

Four 6-32 tapped holes
on 1.950 B.C.
at 45, 135, 225, and 315
degrees

.697   .697

Four 6-32 clearance
holes on 1.950 B.C.
at 0, 90,180 and
270 degrees

.156 thru
two places

A   A

1.50
±.01

Two 6-32 clearance
holes on .750 b.c.
at 90 and 270 degrees
countersunk
for flat head

Four 4-40 tapped
holes on 1.950 B.C.
at approximately
22.5,157.5,
202.5 and 337.5
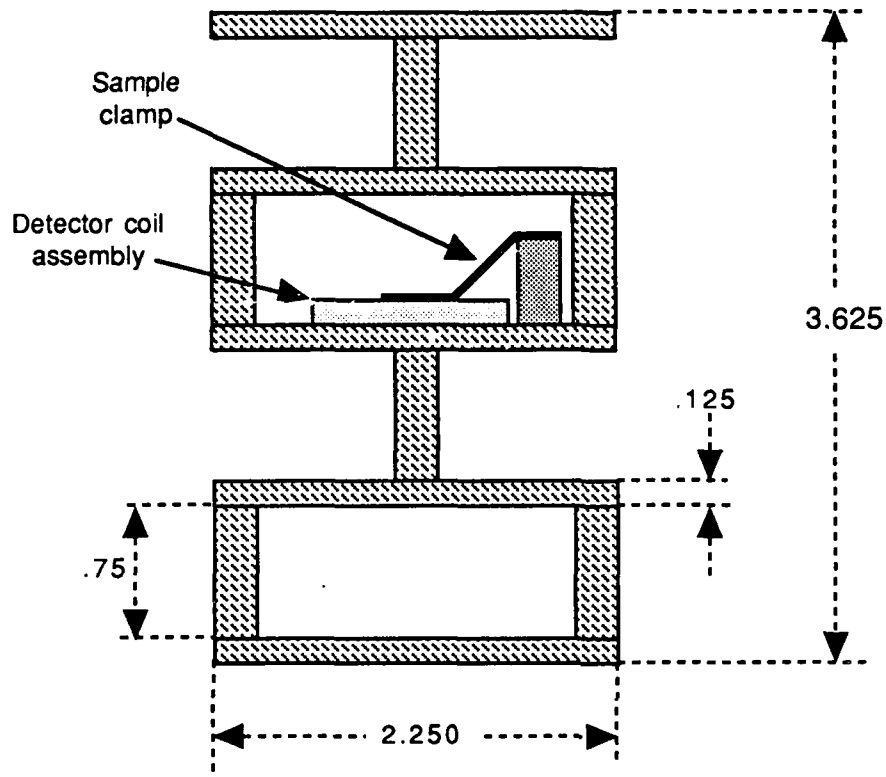degrees

.25
±.01

2.25
±.01

.25 radius

.1875

Cross-section A-A

4-40 tapped holes are used thus: Diode is mounted with one.
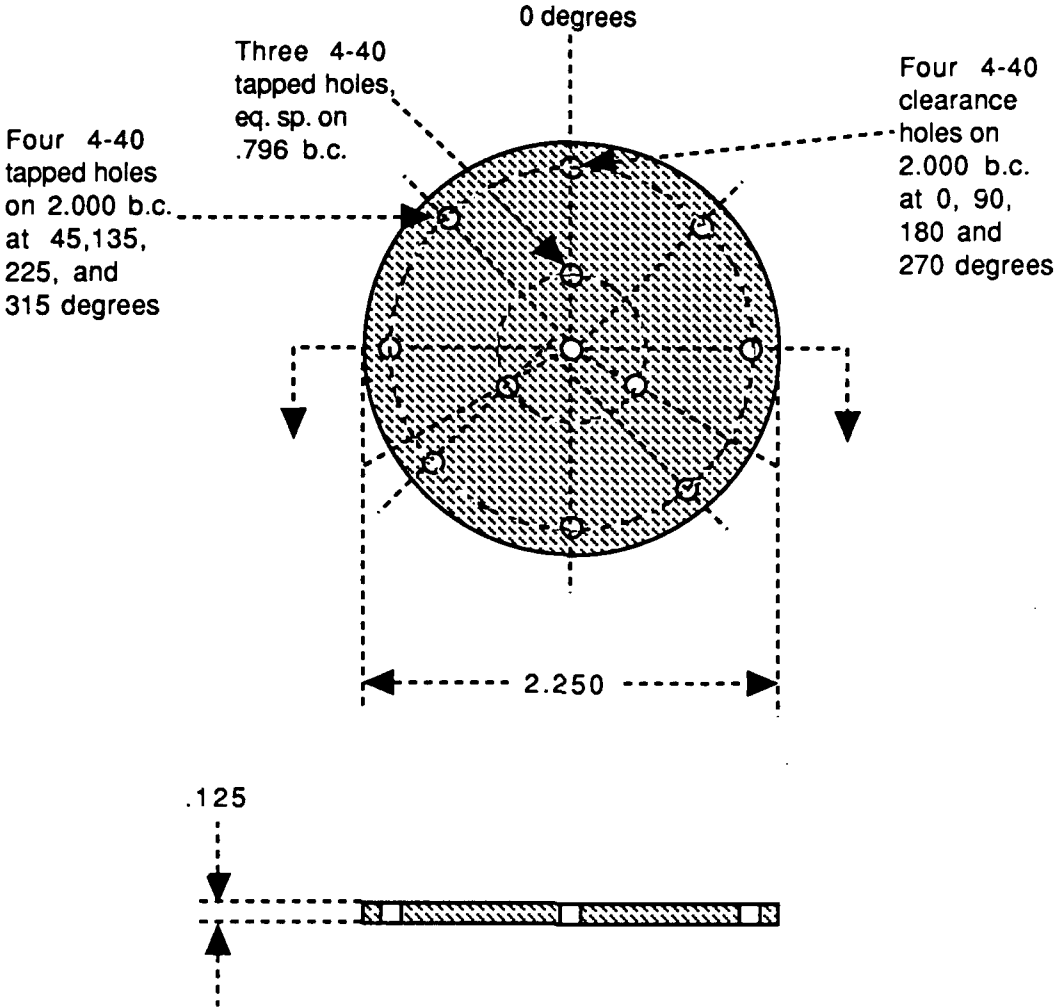Wires are wrapped around brass 4-40 screws in others.

.25 by .125 slot is for pumping out cavity.
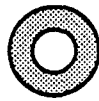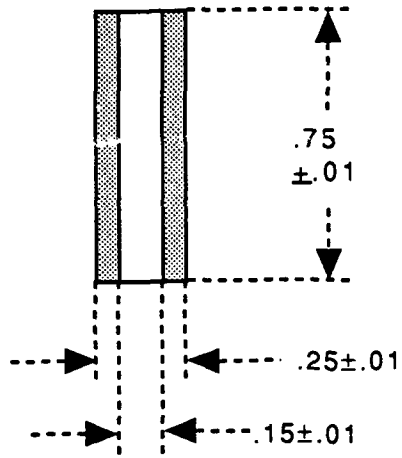
Mounts for Four Coils

Sample clamp

Detector coil assembly

3.625

.125

.75

2.250

Plate for Detector Coil

Mat'l: copper

0 degrees

Three 4-40 tapped holes, eq. sp. on .796 b.c.

Four 4-40 clearance holes on 2.000 b.c. at 0, 90, 180 and 270 degrees

Four 4-40 tapped holes on 2.000 b.c. at 45, 135, 225, and 315 degrees

2.250

.125

Spacer for Mounting Coils

Mat'l: copper

.75
±.01

.25±.01

.15±.01

Post for Sample Clamp

Mat'l: copper

.50±.01

.25±.01

.15±.01
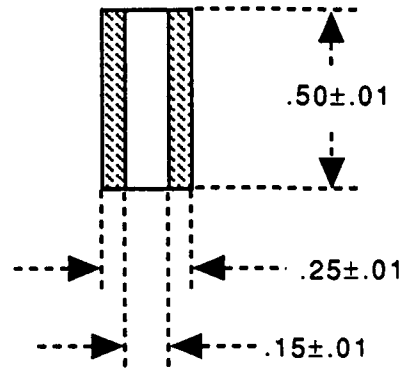
General Atomics TE₀₁₁ Cavity
Dimensions in Inches

Cavity Frame Top

Cavity Body

Cavity Frame Bottom

1.55"

1.45"

1.35"

1.68"

2.25"

Cavity Frame Top

Mat'l: brass

.697 .697

Four 6-32 tapped
holes on 1.950 B.C.
at 0, 90,180 and
270 degrees

1.18±.01
dia. through

Four 6-32 clearance holes
on 1.950 B.C. at 45, 135,
225, and 315 degrees

.156 thru
two places

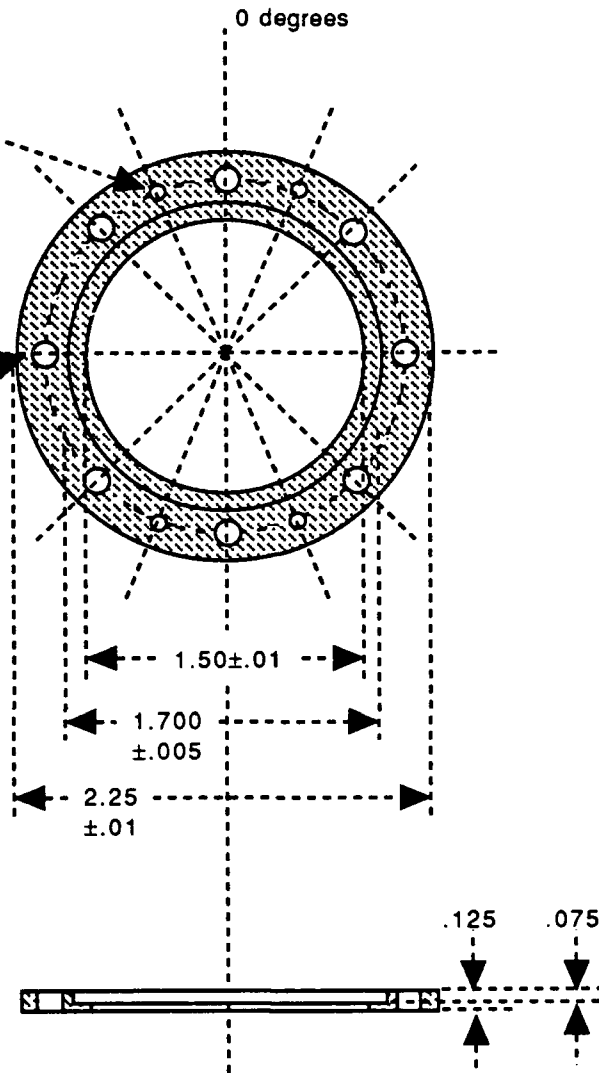1.700
+.000
-.005

2.25
±.01

.125 .075
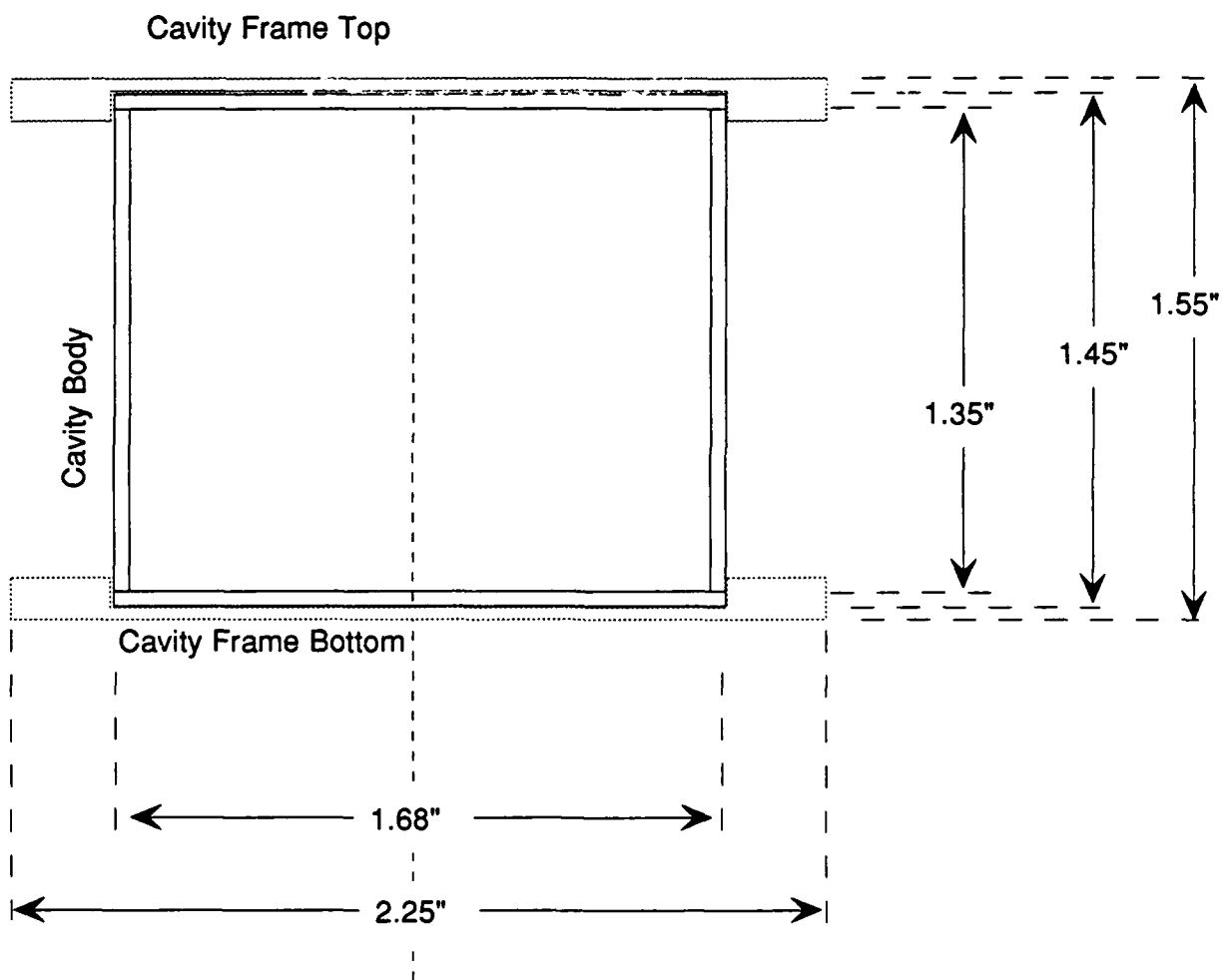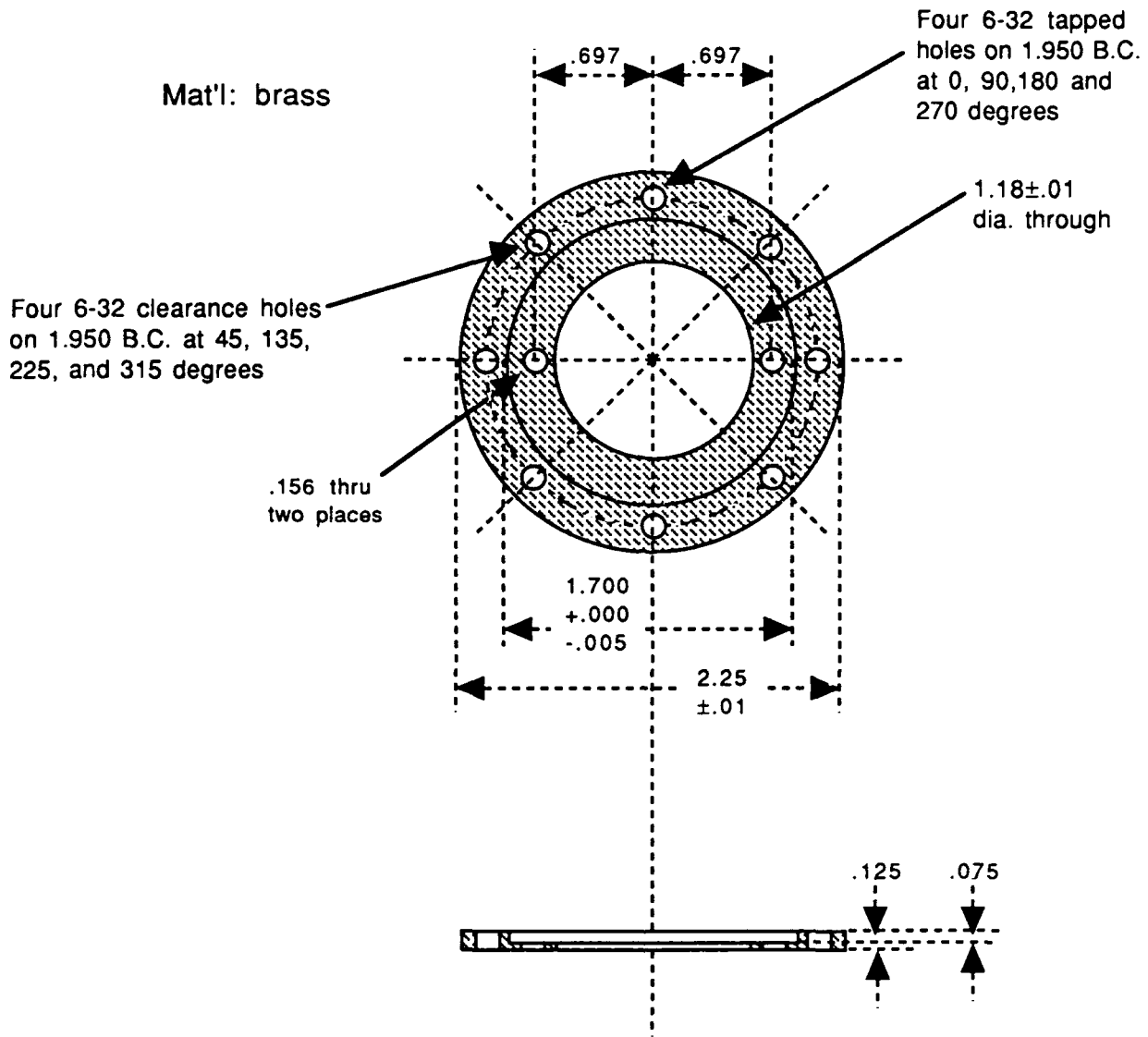
Cavity frame bottom is bolted to this with four 6-32 screws.
This is bolted to the mounting plate with four 6-32 screws.

Cavity Frame Bottom

Mat'l: brass

Four 4-40 tapped holes
on 1.950 B.C.
at approximately
22.5, 157.5, 202.5
and 337.5 degrees.

0 degrees

Eight 6-32
clearance
holes eq. sp.
on 1.950 B.C.

1.50±.01

1.700
±.005

2.25
±.01

.125   .075

This is bolted to the cavity frame top with four 6-32
screws. The 4-40 tapped holes are for mounting a
temperature sensing diode.

A-22